RESEARCH

Taxonomic and molecular characterization of a new entomopathogenic nematode species, *Heterorhabditis casmirica* n. sp., and whole genome sequencing of its associated bacterial symbiont

Aashaq Hussain Bhat[1,2]* , Ricardo A. R. Machado[2], Joaquín Abolafia[3], Alba N. Ruiz-Cuenca[3], Tarique Hassan Askary[4], Fuad Ameen[5] and Wasim Muzamil Dass[6]

Abstract

Background Nematodes of the genus *Heterorhabditis* are important biocontrol agents as they form a lethal combination with their symbiotic *Photorhabdus* bacteria against agricultural insect pests. This study describes a new species of *Heterorhabditis*.

Methods Six *Heterorhabditis* nematode populations were recovered from agricultural soils in Jammu and Kashmir, India. An initial examination using mitochondrial and nuclear genes showed that they belong to a new species. To describe this new species, a variety of analyses were conducted, including reconstructing phylogenetic relationships based on multiple genes, characterizing the nematodes at the morphological and morphometric levels, performing self-crossing and cross-hybridization experiments, and isolating and characterizing their symbiotic bacteria.

Results The newly discovered species, *Heterorhabditis casmirica* n. sp., shares 94% mitochondrial cytochrome C oxidase subunit I gene (*COI*) sequence identity with *Heterorhabditis bacteriophora* and *Heterorhabditis ruandica*, and 93% with *Heterorhabditis zacatecana*. Morphologically, it differs from *H. bacteriophora* in its infective juvenile phasmids (present vs. inconspicuous) and bacterial pouch visibility in the ventricular portion of the intestine (invisible vs. visible); genital papilla 1 (GP1) position (at manubrium level vs. more anterior), and in its *b* ratio (body length/neck length), *c* ratio (tail length/bulb width), and *D*% [(excretory pore/neck length) × 100]. Other morphological differences include anterior end to the nerve ring distance (77–100 vs. 121–130 μm), *V*% [(anterior end of vulva/body length) × 100] (46–57 vs. 41–47) in hermaphroditic females; rectum size (slightly longer than the anal body diameter vs. about three times longer), phasmids (smaller vs. inconspicuous), body length (0.13–2.0 vs. 0.32–0.39 mm), body diameter (73–150 vs. 160–220 μm), anterior end to the excretory pore distance (135–157 vs. 174–214 μm), and demanian ratios in amphimictic females. Morphological differences with *H. ruandica* and *H. zacatecana* were also observed. Furthermore, *H. casmirica* n. sp. did not mate or produce fertile progeny with other *Heterorhabditis* nematodes reported from India. It was also discovered that *H. casmirica* n. sp. is associated with 'Photorhabdus laumondii subsp. *clarkei* symbiotic bacteria.

*Correspondence:
Aashaq Hussain Bhat
aashiqhussainbhat10@gmail.com
Full list of author information is available at the end of the article

Bhat *et al. Parasites & Vectors* (2023) 16:383

Page 2 of 28

Conclusions The discovery of *H. casmirica* n. sp. provides novel insights into the diversity and evolution of *Heterorhabditis* nematodes and their symbiotic bacteria. This new species adds to the catalog of entomopathogenic nematodes in India.

Keywords Entomopathogenic nematodes, Biological control agents, Species description, Nematode morphology, Phylogenetics, Taxonomy, *Photorhabdus*

Background

Entomopathogenic nematodes belonging to the families Heterorhabditidae and Steinernematididae are highly effective biocontrol agents against agricultural pests. These nematodes have independently evolved mutual associations with insect pathogenic bacteria of the genera *Photorhabdus* and *Xenorhabdus*, respectively [1–4]. At the infective juvenile (IJ) stage, these nematodes, which reside in the soil, actively search for insect hosts [5]. When an appropriate host is located, the IJs penetrate the insect body through natural openings or by directly breaking through the cuticle. They then release their bacterial symbionts upon sensing unknown chemical cues in the hemolymph [6, 7]. The bacteria multiply and produce virulence factors and toxins that kill the infected host [8–10]. Furthermore, the bacteria secrete exoenzymes that degrade the insect tissues and produce several metabolites essential for nematode growth, development, and reproduction [11, 12]. The bacteria also produce potent secondary metabolites that act as antibiotics and deter scavenging arthropods. Upon resource depletion, the new generation of nematodes disperses in search of new hosts [9, 13].

Heterorhabditis species are generally more virulent than those of *Steinernema* [14]. However, they are less speciose than *Steinernema* [15, 16]. Despite this, new valid species of *Heterorhabditis* are often described and added to the list. The genus *Heterorhabditis* comprises 21 valid species, including two recently described species, *Heterorhabditis ruandica* from Rwanda and *Heterorhabditis zacatecana* from Mexico [15, 17]. Most of the valid species described so far have been molecularly characterized, except for *Heterorhabditis egyptii* [18] and *Heterorhabditis hambletoni* [19], which have only been morphologically characterized. The genus *Heterorhabditis* is globally distributed, although some species are only reported in certain geographic regions. In India, for instance, three species of *Heterorhabditis* have been documented so far: *Heterorhabditis indica* [20, 21], *Heterorhabditis bacteriophora* [22], and *Heterorhabditis baujardi* [23]. *Heterorhabditis indica*, described by Poinar et al. [20], is the only new species of the genus *Heterorhabditis* reported from India to date.

In this study, we present the discovery of, and characterize, a new entomopathogenic nematode species, *Heterorhabditis casmirica* n. sp., and its symbiotic bacteria, recovered from the union territory of Jammu and Kashmir, India. Our study contributes to the characterization of soil biodiversity in general and advances our efforts to understand the biodiversity of an important group of biological control agents, which are essential tools for eco-friendly and sustainable agricultural practices.

Methods

Nematode origin

Six populations of nematodes, namely HM, HM8, HP1, HPH, HH1, and HH4, were obtained from soil samples collected in the northwestern part of the union territory of Jammu and Kashmir, India. The samples were collected from soils around the roots of walnut and willow trees in the Anantnag district (Global Positioning System coordinates 33.828914, 75.100091; altitude 1606 m above sea level). Each one of these six populations was isolated from different soil samples. Each soil sample was separated by about 2 km from each other. Nematodes were isolated from soil samples using *Corcyra cephalonica* as a bait insect. Insects with nematode infestation symptoms were washed with double distilled H_2O, sterilized with 0.1% $NaOCl_2$, and then placed in White traps to recover the new generation of IJs [24]. Recovered nematodes were reared using *Galleria mellonella* larvae as hosts under laboratory conditions [25, 26]. The IJs were stored in 250-mL tissue culture flasks in a biological oxygen demand incubator at 15 °C [27, 28]. The new species has been registered at ZooBank under urn:lsid:zoobank.org:pub:BBFC7CC6-7294-4548-AA7F-5CD5293E4103.

Nematode morphological and morphometric characterization, light and scanning electron microscopy

Hermaphroditic females, males and amphimictic females were obtained by dissecting *G. mellonella* cadavers in Ringer's solution 4 and 6 days after infestation, respectively [26, 28]. The IJs were collected from White traps after emerging from the *G. mellonella* cadavers. The nematodes were then killed with hot water, fixed in TAF solution (2 mL triethanolamine, 7 mL of 40% commercial

Bhat *et al. Parasites & Vectors* (2023) 16:383

Page 3 of 28

formaldehyde solution, and 91 mL distilled water), transferred to anhydrous glycerin, and mounted on permanent glass slides with additional layers of paraffin wax to prevent flattening during microscopy [29, 30]. Morphological measurements (in micrometers) were taken using Nikon DS-L2 image acquisition software on a phase-contrast microscope (Nikon Eclipse 80i). Twenty specimens at each developmental stage were measured. Light microscopy (LM) and scanning electron microscopy (SEM) photographs were obtained using various nematological techniques detailed by Abolafia [31]. In brief, nematodes fixed in 4% formalin solution were processed to anhydrous glycerin using Siddiqi's method with lactophenol-glycerin solutions [32]. Subsequently, the nematodes were permanently mounted on glass microscope slides using the glycerin-paraffin method [33, 34]. The LM photographs were captured using a Nikon Eclipse 80i microscope (Olympus, Tokyo, Japan) with differential interference contrast optics and a Nikon Digital Sight DS-U1 camera. For SEM, nematodes preserved in glycerin were removed from permanent microscope slides by removing the cover glass, rehydrated in distilled water, dehydrated in a graded ethanol–acetone series, critically point dried with liquid CO_2, mounted on SEM stubs with copper tape, coated with gold in a sputter coater, and finally observed with a Zeiss Merlin microscope (5 kV) (Zeiss, Oberkochen, Germany) [35]. The LM and SEM micrographs, obtained at different magnifications for each structure, were processed and combined using Adobe Photoshop Creative Suite (Microsoft, Redmond, WA).

Comparisons were made between all the valid described species of *Heterorhabditis* based on morphological, morphometric and molecular characters, using the keys published by Machado et al. [17]. Demanian indices and other ratios were calculated following the method outlined by de Man [36]. The stoma morphology was described using the terminology provided by De Ley et al. [37], the spicule and gubernaculum morphology was described using the terminology established by Abolafia and Peña-Santiago [38] and the terminology for pharynx follows the proposals of Bird and Bird [39] and Baldwin and Perry [40].

Self-crossing and cross-hybridization experiments
Self-crossing and cross-hybridization experiments were carried out on lipid agar plates following the methodology described by Dix et al. [41]. *Heterorhabditis casmirica* n. sp. isolates HM, HM8, HP1, HPH, HH1, and HH4 were crossed with each other and allowed to interact with Indian populations of *H. bacteriophora* (P4, P5 and KAS), *H. indica* (TH7, TH8 and TH9) and *H. baujardi* (HeTD4) nematodes. Control experiments were also conducted by self-crossing all the nematode species/strains. In each experiment, 20 second-generation males and 20 second-generation virgin females of each species were placed on 35-mm-diameter lipid agar plates and incubated at 25 °C. Progeny production was observed daily for 7 consecutive days. The experiments were conducted twice under the same conditions.

Nematode molecular characterization and phylogenetic relationships
Genomic DNA was extracted from individual hermaphroditic females isolated from insect cadavers infested with *H. casmirica* n. sp. HM, HM8, HP1, HPH, HH1, or HH4, as described [42]. Briefly, individual virgin females were washed separately with Ringer's solution and then washed in phosphate-buffered saline (pH 7.2). Virgin females were then individually transferred to sterile polymerase chain reaction (PCR) tubes (0.2 mL) containing 20 μL extraction buffer (17.6 μL nuclease-free distilled H_2O, 2 μL of 5X PCR buffer, 0.2 μL 1% Tween, and 0.2 μL proteinase K). Samples were frozen at −20 °C for 60 min or overnight and then immediately incubated in a PCR thermocycler at 65 °C for 1.2 h, followed by incubation at 95 °C for 10 min. The lysates were cooled on ice and centrifuged at 6500 *g* for 3 min. The resulting supernatants were used as DNA templates to amplify different taxonomically relevant gene markers. A fragment of ribosomal rRNA (rRNA) containing the internal transcribed spacer (ITS) regions (ITS1-5.8S-ITS2) was amplified using primers 18S (5′-TTGATTACGTCCCTGCCC TTT-3′) (forward) and 28S (5′-TTTCACTCGCCGTTA CTAAGG-3′) (reverse) [43]. A fragment of rRNA containing the D2–D3 regions of the 28S rRNA was amplified using primers D2F (5′-CCTTAG TAACGGCGA GTGAAA-3′) (forward) and 536 (5′-CAGCTATCCTGA GGAAAC-3′) (reverse) [44]. The 12S mitochondrial gene was amplified using primers 505F (5′-GTTCCAGAA TAATCGGCTAGAC-3′) (forward) and 506R (5′-TCT ACTTTACTACAACTTACT CCCC-3′) (reverse) [44] and the mitochondrially encoded cytochrome oxidase subunit I gene (*MT-COI*) was amplified using primers HCF (5′-TTACATGATACTTATTATG-3′) (forward) and HCF (5′-CTGATAACTGTGACCAAATACATA -3′) (reverse) [45]. The PCR reactions consisted of 2 μL of DNA extract, 12.5 μL of DreamTaq Green PCR Master Mix (Thermo Scientific, USA), 0.75 μL of each forward and reverse primer at 10 μM and 9 μL of nuclease-free distilled H_2O. The PCR reactions were performed using a thermocycler (Applied Biosystems Veriti 96-Well Thermal Cycler) with the following settings: (i) for ITS, D2–D3 and 12S—one cycle of 3 min at 94 °C followed by 35 cycles of 30 s at 94 °C, 30 s at 50 °C, 1 min 30 s at 72 °C, followed by a single final elongation step at 72 °C for

Bhat *et al. Parasites & Vectors* (2023) 16:383

Page 4 of 28

20 min; (ii) for the *MT-COI* gene—one cycle of 3 min at 94 °C followed by 38 cycles of 10 s at 94 °C, 30 s at 40 °C, 60 s at 72 °C, followed by a single final elongation step at 72 °C for 10 min [46]. PCR was followed by electrophoresis (45 min, 100 V) of 5 µL of PCR products in a 1% Tris–boric acid–ethylenediaminetetraacetic acid-buffered agarose gel stained with SYBR Safe DNA Gel Stain (Invitrogen, Carlsbad, CA). PCR products were purified using the FastGene Gel/PCR extraction kit (Nippon Genetics, Japan) and sequenced using reverse and forward primers by Sanger sequencing (Bioserve, Hyderabad, India). The obtained sequences were manually curated, trimmed and deposited at the National Center for Biotechnology Information (NCBI) under the accession numbers given in Additional file 1: Table S4. To complete this data set and to obtain genomic sequences of nematodes that belong to all the valid described species of the genus *Heterorhabditis*, we searched the database of the NCBI by using the Basic Local Alignment Search Tool and the accession numbers of the sequences obtained previously [17, 47]. The resulting sequences were used to reconstruct phylogenetic relationships by the maximum likelihood method based on the following nucleotide substitution models: Tamura–Nei (TN93+G+I) (*MT-COI*) and Kimura 2-parameter (K2+G) (D2–D3) (ITS). To select the best substitution models, best-fit nucleotide substitution model analyses were carried out in MEGA 11 [48–51]. Sequences were aligned with MUSCLE (v3.8.31) [52]. The trees with the highest log likelihood are shown. The percentage of trees in which the associated taxa clustered is shown next to the branches. Initial tree(s) for the heuristic search were obtained automatically by applying neighbor–joining and BIONJ algorithms to a matrix of pairwise distances estimated using the maximum composite likelihood approach, and selecting the topology with a superior log-likelihood value. In some cases, a discrete gamma distribution (+G) was used to model evolutionary rate differences between sites, and the rate variation model allowed for some sites to be evolutionarily invariable (+I). The trees are drawn to scale, with branch lengths measured in the number of substitutions per site. Graphical representation and edition of the phylogenetic trees were performed with Interactive Tree of Life v3.5.1 [53, 54].

Symbiotic relationships

The *Photorhabdus* entomopathogenic bacteria associated with the different *H. casmirica* n. sp. nematode populations were isolated as described previously [55, 56].

Briefly, larvae of *G. mellonella* (Lepidoptera: Pyralidae) were exposed to 100 nematode IJs. Three to 4 days later, insect cadavers were surface sterilized and cut open with a surgical blade. Bacteria-digested internal organs were spread onto Luria—Bertani (LB) agar plates and incubated at 28 °C for 24–48 h. *Photorhabdus*—like colonies were then streaked on fresh LB agar plates until monocultures were obtained. A single primary form colony was then selected and used for further experiments. Bacteria primary forms were determined by examining colony morphology, colony texture, pigment production, and bioluminescence. The strains were further subcultured and maintained on LB agar plates at 28 °C. An initial molecular characterization, using 16S rRNA gene sequences, was carried out to determine the taxonomic affiliation of the obtained bacterial cultures as described previously [3, 4, 17, 56]. Phylogenetic reconstruction and sequence comparisons based on whole genome sequences were carried out to confirm the taxonomic affiliation of the obtained bacterial cultures as described previously [3, 55, 56]. Briefly, genomic DNA was extracted and purified using the GenElute Bacterial Genomic DNA Kit (Sigma-Aldrich, Switzerland) following the manufacturer's instructions. The resulting DNA was used for library preparation using the TruSeq DNA PCR-Free LT Library Prep (FC-121-3003) kit. Indexed libraries were then pooled at equimolar concentrations and sequenced [2×150 base pairs (bp)] on an Illumina HiSeq 3000. Raw Illumina reads were quality trimmed using Trimmomatic 0.39 [57]. The resulting reads were assembled with SPAdes 3.14.1 (*k*-mer sizes of 31, 51, 71, 91, and 111 bp) [58]. Scaffolds with a mean read depth smaller than 20% of the median read depth of the longer scaffolds ($\geq$ 5000 bp) as well as scaffolds that were shorter than 200 bp were removed. The final assemblies were polished using Pilon 1.22 [59]. Phylogenetic relationships were reconstructed based on the assembled genomes and the genome sequences of all valid published species of the genus [3, 55, 56]. For this, core genome alignments were created using Roary 3.6.2 [60]. Based on this alignment, a maximum likelihood tree was constructed using Fasttree 2.1.10 based on the Jukes–Cantor plus CAT nucleotide evolution model [61].

Results and discussion

Six populations of *Heterorhabditis* nematodes (HM, HM8, HP1, HPH, HH1, and HH4) were isolated from agricultural soils in Kashmir, India. Initial molecular and
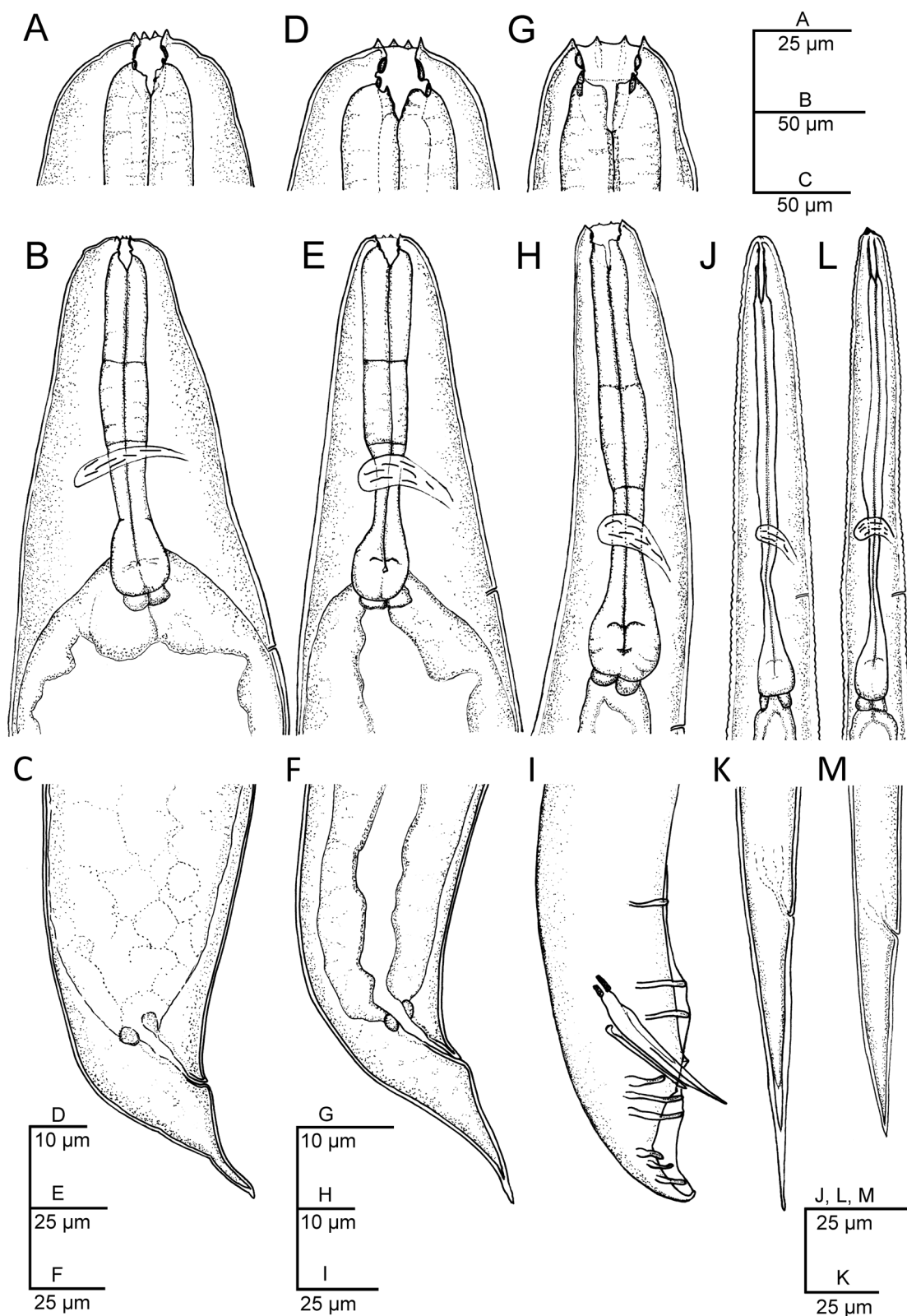
Fig. 1 a–m *Heterorhabditis casmirica* n. sp. (drawings). **a**, **d**, **g** Anterior end of hermaphroditic female, amphimictic female and male, respectively. **b**, **e**, **h**, **j**, **l** Neck region of hermaphroditic female, amphimictic female, male, second-stage juvenile (J2) and third-stage juvenile (J3), respectively. **c**, **f**, **i**, **k**, **m** Posterior end of hermaphroditic female, amphimictic female, male, J2 and J3, respectively

Bhat *et al. Parasites & Vectors* (2023) 16:383

Page 6 of 28
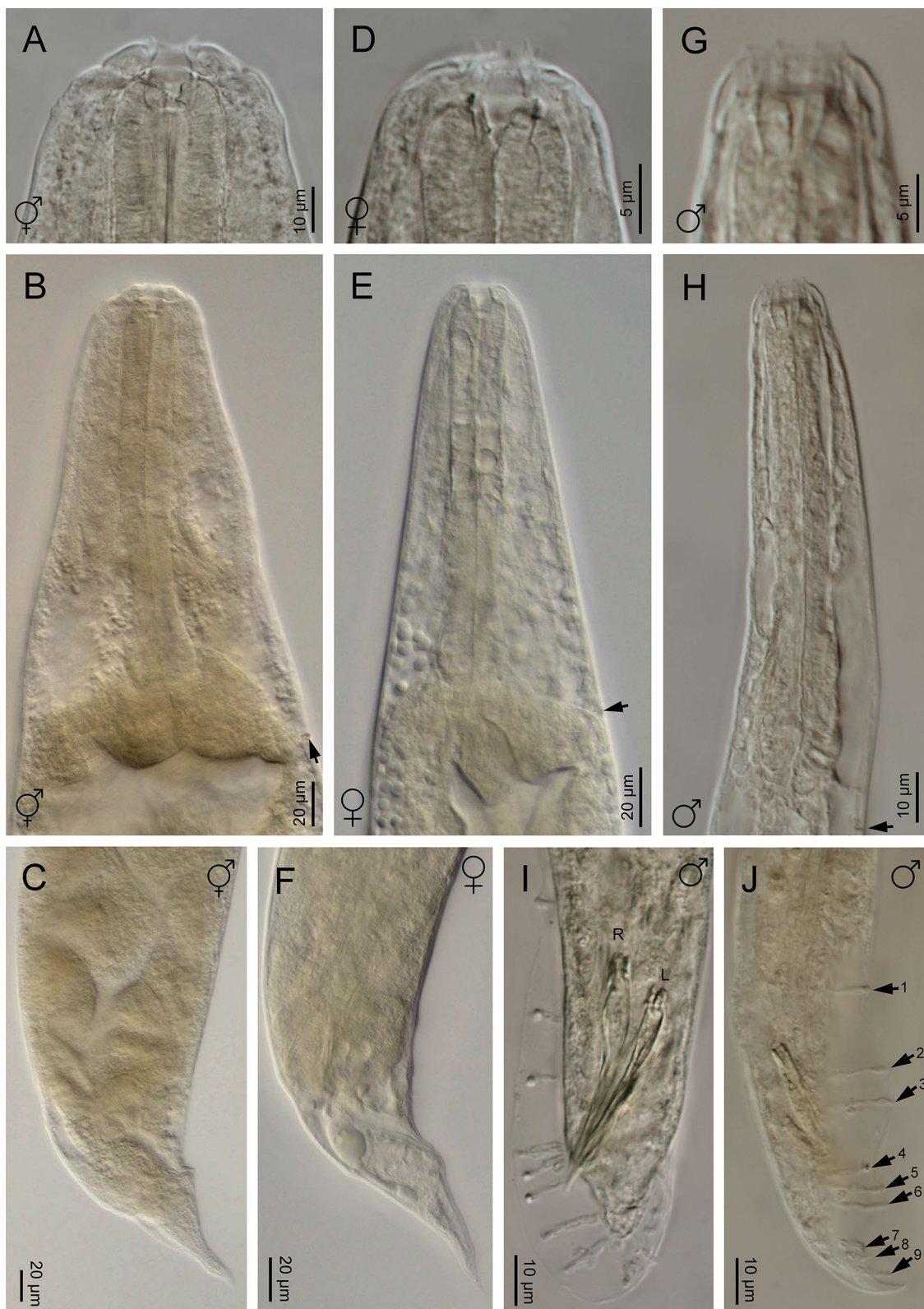
Fig. 2 **a**–**j** *Heterorhabditis casmirica* n. sp. (light microscopy images). **a**, **d**, **g** Anterior end of hermaphroditic female, amphimictic female and male, respectively. **b**, **e**, **h** Neck region of hermaphroditic female, amphimictic female and male, respectively (arrowhead indicates the excretory pore). **c**, **f** Posterior end of hermaphroditic female and amphimictic female, respectively. **i**, **j** Posterior end of male at spicule and bursa levels, respectively [arrowhead indicates the genital papillae (GP)]

Bhat *et al. Parasites & Vectors* (2023) 16:383

Page 7 of 28
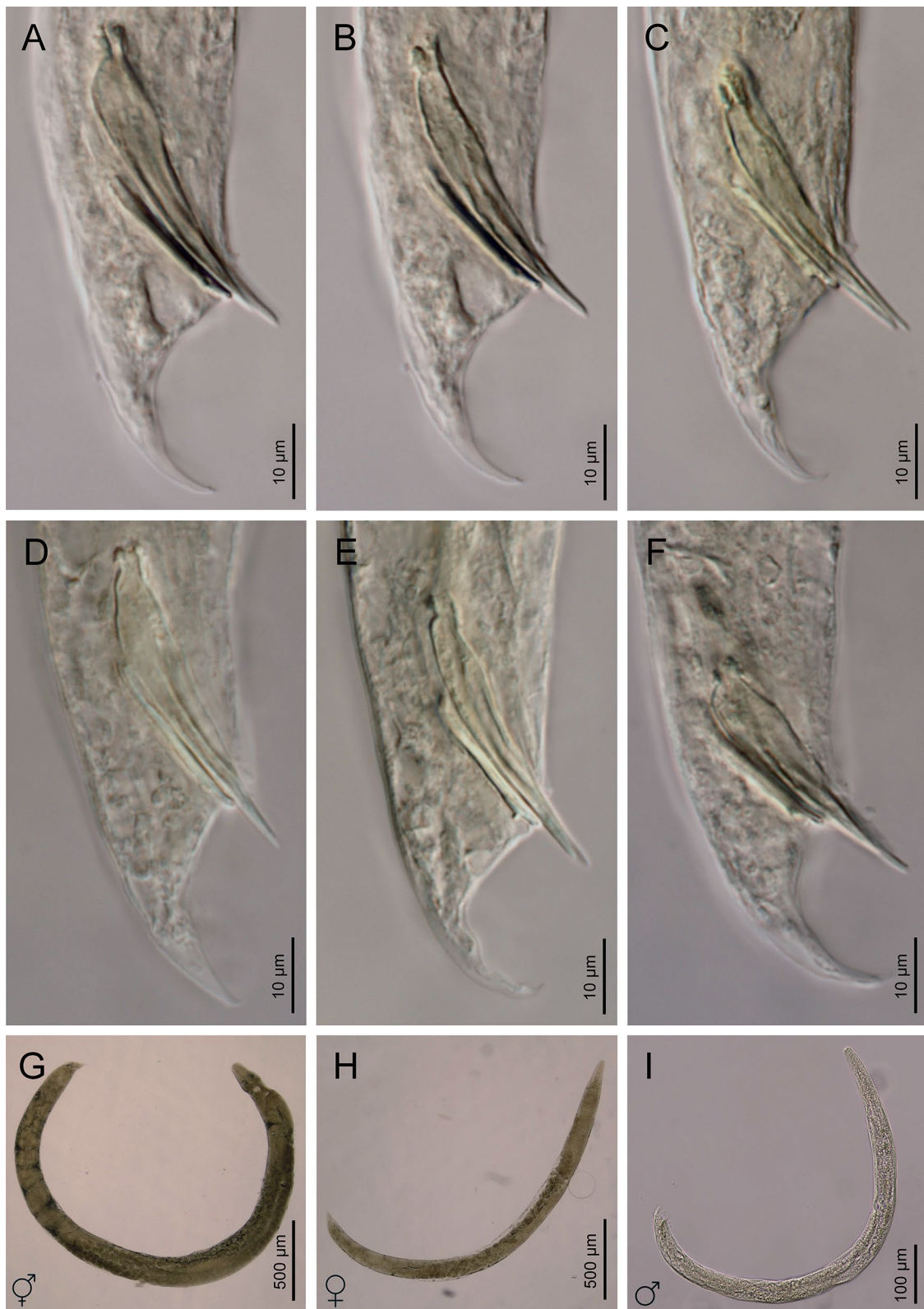
Fig. 3 **a**–**i** *Heterorhabditis casmirica* n. sp. (light microscopy images). **a**–**f** Spicule and gubernaculum variability. **g** Hermaphroditic female. **h** Amphimictic female. **i** Male

Bhat *et al. Parasites & Vectors* (2023) 16:383

Page 8 of 28
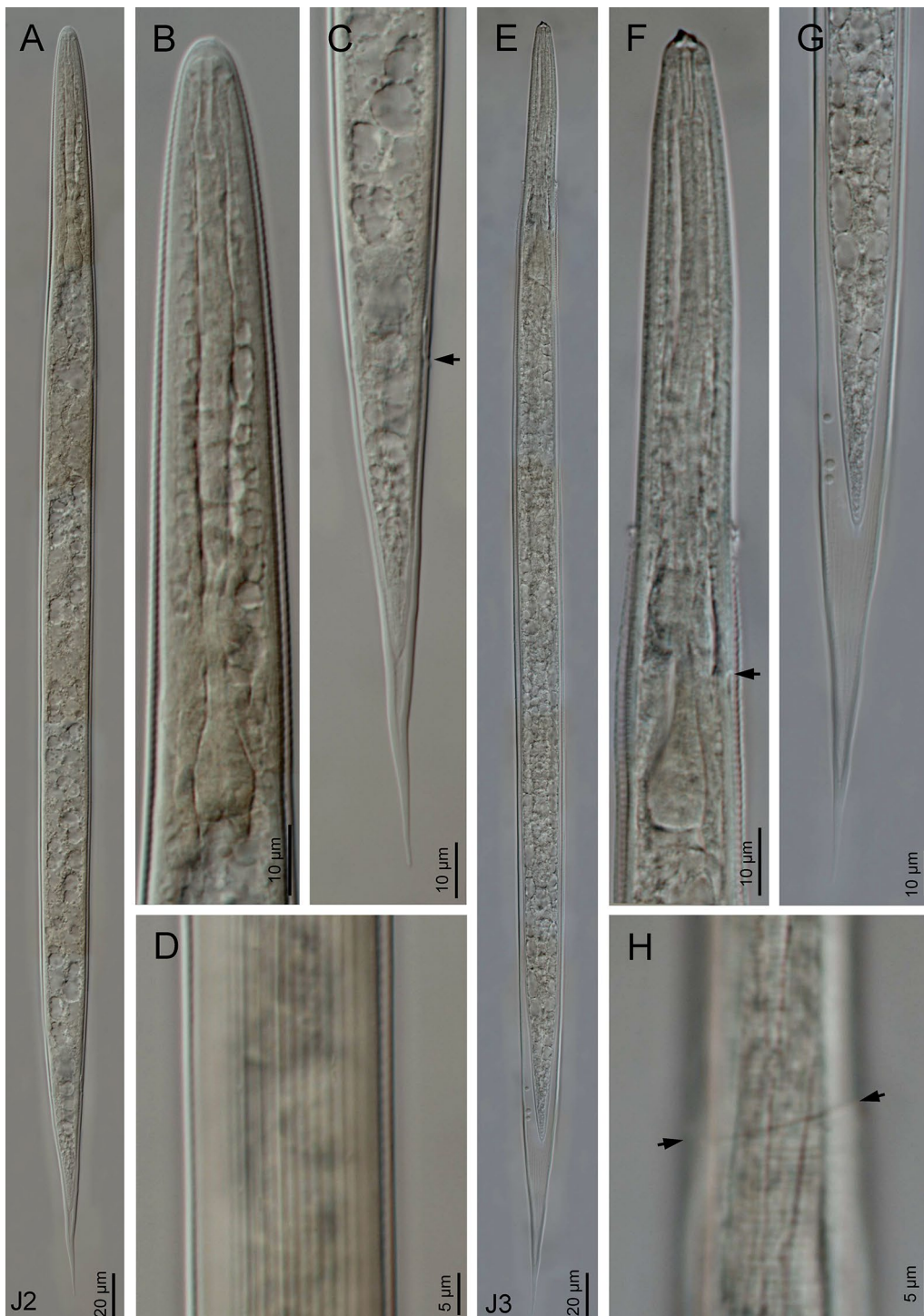
Fig. 4 **a–h** *Heterorhabditis casmirica* n. sp. (light microscopy images). **a**, **e** Entire body of J2 and J3, respectively. **b**, **f** Neck region of J2 and J3, respectively (arrowhead indicates the excretory pore). **c**, **g** Posterior end of J2 and J3, respectively (arrowhead indicates the anus). **d**, **h** Cuticle of J2 and J3, respectively (arrowheads indicate the lateral field)

Bhat *et al. Parasites & Vectors* (2023) 16:383

Page 9 of 28

morphological characterization showed that they are genetically identical, morphologically very similar, and represent a novel species closely related to *H. bacteriophora*. The nematode population HM was chosen as the type material to describe this newly discovered species.

Heterorhabditis casmirica n. sp.

Morphological and morphometric characteristics of *H. casmirica* n. sp are presented in Figs 1, 2, 3, 4, 5, 6 and Tables 1, 2, 3, 4, 5.

Hermaphroditic females

Hermaphroditic female body C-shaped when heat relaxed, body robust, always containing many juveniles, in some specimens a few eggs were visible. Cuticle almost smooth, about 0.8 to 1.6 µm thick. Lateral fields and phasmids not distinguishable under LM. Anterior end tapering anteriorly. Labial region with six prominent lips, each with a terminal conoid labial papilla. Cephalic papillae not observed with LM. Amphidial apertures pore-like. Stoma rhabditoid type, 1.1–1.7 times the lip region width, with a short cheilostom with a hardly visible refringent rounded cheilorhabdia, gymnostom with refringent bar-like rhabdia, well-developed, and funnel-shaped stegostom surrounded by the pharyngeal collar and bearing minute rhabdia. Pharynx with sub-cylindrical procorpus, slightly swollen metacorpus, robust isthmus, and poorly developed, spheroid basal bulb with inconspicuous valves. Nerve ring surrounding the isthmus, at 55–74% of neck length. Excretory pore at basal bulb level or intestine level, at 94–120% of neck length. Cardia conoid. Reproductive system didelphic–amphidelphic. Ovaries well developed, reflexed. Oviducts poorly differentiated. Uteri with numerous embryonated eggs. Vagina short. Vulva a transverse slit, with smooth top and scarcely prominent lips, close to mid-body. Rectum slender, about 0.9–1.4 times the anal body diameter. Anal region swelling posteriorly. Tail conoid with narrower pointed terminus, lacking a mucron. Phasmids inconspicuous.

Amphimictic females

Body arcuate with general morphology similar to that of hermaphroditic females. Body tapering toward anterior end; labial papillae acute and prominent. Reproductive system didelphic–amphidelphic with ovaries well developed, reflexed, oviducts and uteri poorly visible, vagina very short, and vulva small with a transverse slit opening. Rectum slightly longer than that of hermaphroditic females, about 1.7–1.9 times longer than the anal body diameter. Anal lips usually prominent. Tail conoid longer than that of hermaphroditic females, with acute tip lacking a mucron. Phasmids very small, located at 50–62% of tail length.

Males

Body curved ventrally (open C-shape) or sometimes straight when heat relaxed. Anterior end truncate. Lip region with six scarcely separated lips and six conoid liplets at oral margin; six labial papillae at liplet tips and four cephalic papillae at the base of the dorsal and ventral lips. Amphidial aperture pore-like, just posterior to the lateral lips. Stoma 0.8–1.4 times the lip region width, with short cheilostom and hardly visible refringent rounded cheilorhabdia, short gymnostom with refringent bar-like rhabdia, and long, funnel-shaped stegostom surrounded by the pharyngeal collar and bearing minute rhabdia. Pharynx with subcylindrical procorpus, scarcely swollen metacorpus, isthmus robust and slightly narrower than metacorpus, and basal bulb poorly developed, spheroid, with poorly developed valvular apparatus. Nerve ring located surrounding isthmus, at 55–69% of neck length. Excretory pore located at basal bulb or intestine level, at 99–107% of neck length. Cardia conoid, protruding into intestine. Intestine without differentiation although with narrower walls at anterior end. Reproductive system monorchid, with testis anteriorly reflexed and vas deferens well developed. Spicules well developed, separate, with small, almost quadrangular manubrium with very refringent dorsal and ventral walls, frequently smaller at the left spicule, calamus developed, and almost straight lamina with acute tip, poorly developed dorsal hump, and ventral velum slightly developed. Gubernaculum robust,

(See figure on next page.)

Fig. 5 **a**–**n** *Heterorhabditis casmirica* n. sp. (scanning electron microscopy images). **a**, **f**, **k** Lip region (frontal view) in hermaphroditic female, amphimictic female and male, respectively (arrowheads indicate the amphids). **b**, **g**, **l** Lip region in hermaphroditic female (ventral view), amphimictic female (lateral view) and male (sublateral view), respectively (arrowheads indicate the amphids). **c** Vulva of hermaphroditic female. **d**, **i** Tail (lateral view) in hermaphroditic female and amphimictic female, respectively (arrowheads indicate the phasmid). **e**, **j** Tail (ventral view) in hermaphroditic female and amphimictic female, respectively. **h** Excretory pore (arrowhead) of amphimictic female. **m**, **n** Male posterior end (lateral and ventral views, respectively) (arrowheads indicate the bursal papillae)

Bhat *et al. Parasites & Vectors* (2023) 16:383

Page 10 of 28
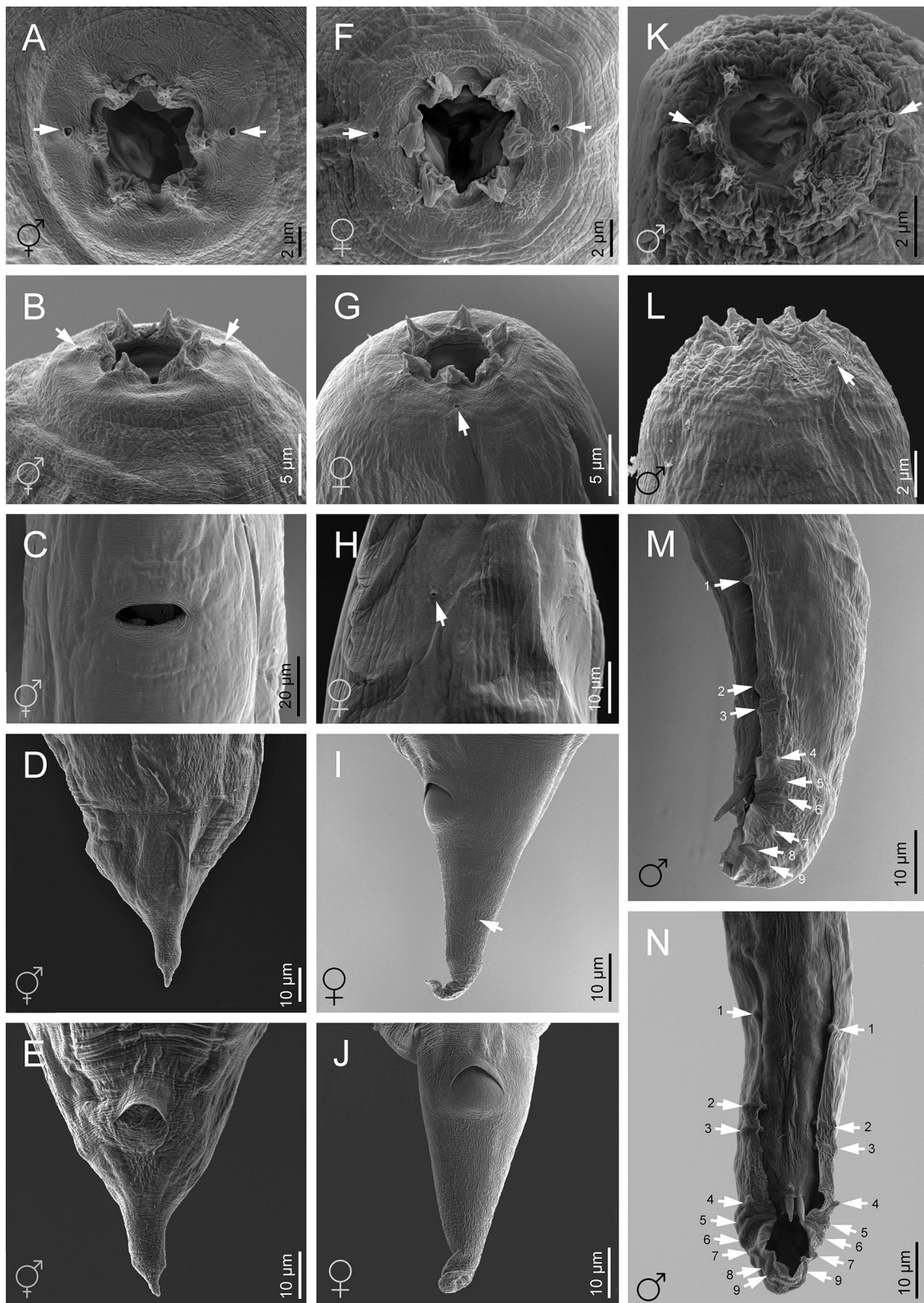
Fig. 5 (See legend on previous page.)

Bhat *et al. Parasites & Vectors* (2023) 16:383

Page 11 of 28
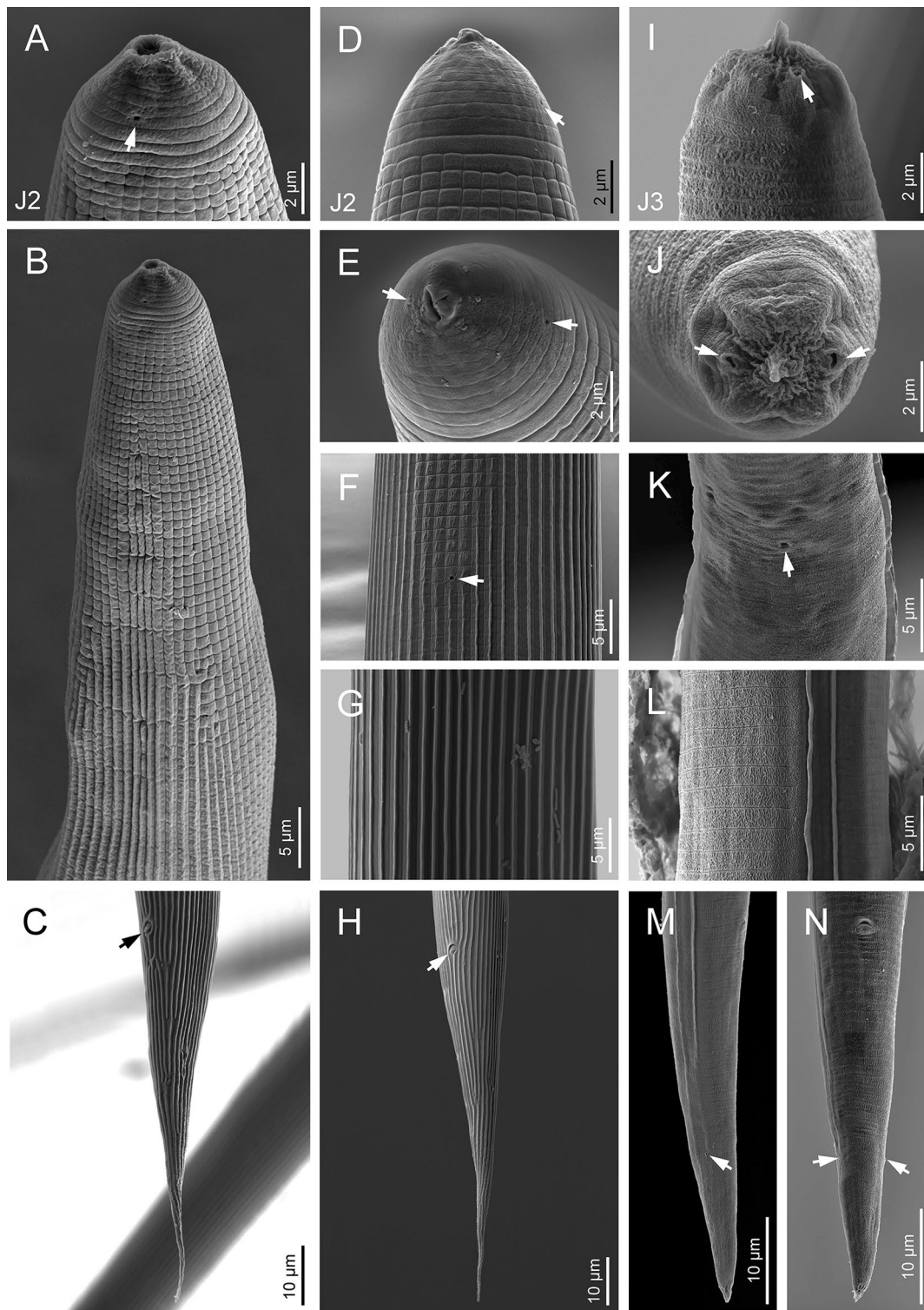
Fig. 6 **a**–**n** *Heterorhabditis casmirica* n. sp. (scanning electron microscopy images). **a**, **d**, **e** Lip region of J2 (lateral, dorsal and frontal views, respectively) (arrowheads indicate the amphids). **b** Neck region of J2. **c**, **h** Tail of J2 (lateral and ventral views, respectively). **f** Excretory pore (arrowhead) of J2. **g** Cuticle at the mid-body region of J2. **i**, **j** Lip region of J3 (lateral and frontal views, respectively) (arrowheads indicate the amphids). **k** Excretory pore (arrowhead) of J3. **l** Lateral field of J3. **m**, **n** Tail of J3 (lateral and ventral views, respectively) (arrowheads indicate the phasmids)

Bhat *et al. Parasites & Vectors* (2023) 16:383

Page 12 of 28

Table 1 Morphometrics of the infective juvenile (*IJ*) and adult generations of *Heterorhabditis casmirica* n. sp. (population HM)

Characters	Male (holotype)	Males (paratypes)	Hermaphrodites (paratypes)	Females (paratypes)	IJs (paratypes)
n	1	20	20	20	20
Body length (L)	875.5	754±80 (608–914)	3466±392 (2851–4219)	1432±172 (1273–1990)	563±22 (512–599)
a (L/BD)	18.3	18±2.8 (15–24)	24±3.2 (19–27)	20±1.9 (14–25)	23±1.1 (20–25)
b (L/NL)	7.6	7.3±0.4 (6.4–8.2)	24±4.6 (16–39)	11±0.8 (10–13)	4.5±0.2 (4.0–5.2)
c (*L/T*)	30.5	29±3.8 (24–35)	72±32 (56–84)	19±3.2 (16–31)	5.4±0.5 (4.7–6.4)
c′ (T/ABD)	1.3	1.2±0.2 (1.1–1.6)	1.8±0.2 (1.4–2.2)	1.9±0.1 (1.6–2.5)	6.0±0.7 (5.1–8.0)
V% (VA/L×100)	–[a]	–	52±2.7 (46–57)	49±2.1 (45–52)	–
Maximum body diameter (BD)	46.2	36±7.4 (24–48)	230±50 (140–341)	91±17 (70–135)	20±1.0 (17–24)
Excretory pore—anterior end (EP)	83.9	114±4.3 (102–120)	194±8.5 (180–211)	146±7.5 (135–157)	106±6 (98–129)
Width at excretory pore (WEP)	27.8	24±3.2 (19–29)	93±12.2 (71–108)	49±5.6 (41–61)	18±1.3 (14–24)
Nerve ring—anterior end (NR)	60.3	72±6.1 (58–80)	86±9.1 (77–100)	95±6.3 (84–111)	89±4.3 (79–94)
Pharynx length (PL)	98.5	108±7.8 (96–114)	186±9.0 (168–202)	137±7.6 (126–149)	116±5.1 (99–127)
Neck length (NL)	111.7	112±8.2 (100–118)	191±9.5 (174–207)	141±8.3 (132–156)	119±5.4 (104–132)
Bulb length (BL)	16.9	18±2.2 (14–23)	34±2.8 (28–40)	28±2.2 (25–33)	15±1.3 (12–19)
Bulb width (BW)	13.7	12±1.3 (10–15)	26±1.4 (22–30)	20±1.6 (18–23)	8.5±1.6 (6.7–13)
Tail length (*T*)	28.6	25±4.5 (16–32)	82±12 (72–114)	75±5.9 (64–83)	99±7.8 (85–115)
Anal body diameter (ABD)	22.5	18±3.1 (14–25)	44±4.4 (36–56)	26±2.0 (22–30)	15±1.7 (11–20)
Spicule length (SL)	43.5	41±2.9 (38–48)	–	–	–
Gubernaculum length (GL)	23.8	22±2.0 (18–26)	–	–	–
D% (EP/NL×100)	96.4	102±2.3 (99–107)	102±4.8 (94–120)	103±4.0 (99–116)	90±3.8 (83–97)
E% (EP/T×100)	295.3	325±31 (268–394)	236±23 (205–292)	177±15 (156–209)	115±9.1 (93–125)
SW% (SL/ABD×100)	193.2	212±27 (160–252)	–	–	–
GS% (GL/SL×100)	54.6	53±4.3 (45–63)	–	–	–
Body width at vulva	–	–	182±17 (152–218)	90±17 (70–132)	–
Vulva—anterior end (VA)	–	–	1545±152 (1312–1883)	708±80 (631–918)	–
Vulva—posterior end (VP)	–	–	1918±182 (1466–2429)	726 107 (617–1076)	–

All data, with the exception of *n*, ratios and percentages, are given in micrometers, and are shown as the mean±SD (range)

[a] Dashes indicate that these characters are absent in these generations

straight or slightly curved ventrally, 40–63% of spicule length, with manubrium visibly hook-like. Tail conoid with acute tip, ventrally curved posteriorly, flanked by the bursa. Bursa peloderan bearing nine pairs of bursal papillae 1+2/3+3: three precloacal and six postcloacal, with genital papilla 4 (GP4) and genital papilla 7 (GP7) open outside.

Infective sheathed juveniles (third-stage juvenile ensheathed in cuticle of second-stage juvenile)

Body straight when heat relaxed. Sheath (second-stage cuticle) present. Cuticle with longitudinal ridges except for the anterior part of the body, with annuli at the lip region and with tessellate pattern posterior to the lip region. Lip region lacking differentiated lips, bearing six labial papillae and cephalic papillae not visible. Amphidial aperture pore-like, having a cuticular dimple-like structure at its anterior part. Oral opening triradiate, closed. Stoma tubular, about twice as wide as the lip region. Pharynx slender, with corpus subcylindrical, isthmus

narrower and slender, and basal bulb pyriform without developed valves. Nerve ring surrounding the isthmus, at 64–76% of neck length. Excretory pore at isthmus level, at 81–94% of neck length. Hemizonid clearly visible. Cardia conoid, surrounded by the intestinal tissue. Bacterial pouch not visible. Lateral fields not well differentiated from cuticle. Rectum narrow, not clearly discernible. Anus not well developed. Tail conoid-elongate with finely rounded terminus, without mucron. Terminal hyaline part 30–45% of tail length. Phasmids not visible.

Infective non-sheathed juveniles (third-stage juvenile)

Body with habitus straight when heat relaxed. Cuticle with transversal striae (annuli). Lateral field with two prominent longitudinal ridges. Lip region rounded, lacking differentiated lips, and labial and cephalic papillae not visible. Amphidial apertures oval. Oral opening rounded, closed, bearing a small dorsal tooth. Stoma, pharynx, nerve ring and excretory pore location similar to the sheathed stage. Hemizonid well developed. Cardia

Bhat *et al. Parasites & Vectors* (2023) 16:383

Page 13 of 28

Table 2 Comparative morphometrics of *Heterorhabditis* IJs

Species	L	BD	EP	NR	NL	T	a	b	c	c'	D%	E%	Country	References
Heterorhabditis amazonensis	567–612	20–24	89–115	76–93	107–132	98–115	24–29	4.4–5.5	5.1–6.1	7.3[b]	83–92	89–109	Brazil	Andaló et al. [65]
Heterorhabditis atacamensis	578–666	19–26	101–126	79–101	124–144	94–107	25–31	4.8–5.7	5.7–7.1	5.7[b]	79–94	149–182	Chile	Edgington et al. [66]
Heterorhabditis bacteriophora	512–671	18–31	87–110	72–93	100–139	83–112	17–30	4.0–5.1	5.7–7.0	6.0[b]	76–92	103–130	Australia	Poinar [62]
Heterorhabditis baujardi	497–595	18–22	91–103	75–86	107–120	83–97	26–30	4.5–5.1	6.0–6.7	7.2[b]	78–88	98–114	Vietnam	Phan et al. [67]
Heterorhabditis beicherriana	566–687	21–25	100–122	85–106	118–146	86–111	24–29	4.2–4.9	5.9–6.8	6.0–7.4	80–93	103–121	China	Li et al. [63]
Heterorhabditis casmirica n. sp.	512–599	17–24	98–129	79–94	114–138	85–115	20–25	4.0–5.2	4.7–6.4	5.1–8.0	83–97	93–136	India	This study
Heterorhabditis downesi	588–692	15–22	96–128	96–105	126–141	62–74	29–42	4.4–5.3	8.5–10.5	4.4[b]	76–96	160–180	Ireland	Stock et al. [68]
Heterorhabditis egyptii	484–515	18–23	81–94	78–100	100–119	53–75	20–27	4.2–5.2	6.8–9.1	6.9[b]	74–82	100–170	Egypt	Abd-Elgawad & Ameen [18]
Heterorhabditis floridensis	554–609	19–23	101–122	68–107	123–142	91–113	25–32	3.9–4.9	5.3–6.6	7.2[b]	71–90	95–134	USA	Nguyen et al. [69]
Heterorhabditis georgiana	547–651	17–26	97–113	74–94	110–139	86–108	23–34	4.1–5.3	5.5–6.9	6.8[b]	70–93	106	USA	Nguyen et al. [64]
Heterorhabditis hambletoni	–[a]	–	–	–	–	–	–	–	–	–	–	–	Brazil	Pereira [19]
Heterorhabditis indica	479–573	19–22	88–107	72–85	109–123	93–109	25–27	4.3–4.8	4.5–5.6	–	79–90	83–103	India	Poinar et al. [20]
Heterorhabditis marelatus	588–700	24–32	81–113	83–113	121–139	99–117	21–29	4.7–5.4	5.5–6.6	3.0[b]	60–86	89–110	USA	Liu & Berry [70]
Heterorhabditis megidis	736–800	27–32	123–142	104–115	147–160	112–128	23–38	4.6–5.9	6.1–6.9	6.3[b]	81–91	103–120	USA	Poinar et al. [71]
Heterorhabditis mexicana	530–620	20–24	83–109	74–88	104–142	91–106	24–28	4.2–5.1	5.5–6.3	8.3[b]	72–86	87–111	Mexico	Nguyen et al. [72]
Heterorhabditis noenieputensis	484–578	21–25	88–105	69–96	79–115	78–95	21–27	4.3–5.2	5.5–6.8	3.4–4.3	81–95	99–125	S. Africa	Malan et al. [73]
Heterorhabditis ruandica	496–591	18–27	70–89	52–64	75–102	49–64	20–29	5.1–6.6	7.6–8.6	3.4–5.8	65–98	99–157	Rwanda	Machado et al. [17]
Heterorhabditis safricana	550–676	19–23	103–122	86–101	125–141	86–108	25–32	3.9–4.9	5.4–7.5	8.7[b]	80–90	99–133	S. Africa	Malan et al. [74]
Heterorhabditis taysearae	332–499	17–23	74–113	58–87	96–130	44–70	18–27	3.4–4.2	6.5–8.7	3.7[b]	71–96	110–230	Egypt	Shamseldean et al. [75]
Heterorhabditis zacatecana	493–578	23–27	72–99	69–72	78–99	52–63	19–24	5.3–7.2	8.2–10	4.3–6.7	72–122	128–184	Mexico	Machado et al. [17]
Heterorhabditis zealandica	570–740	22–30	94–123	90–107	135–147	87–119	25	4.9	6.7	–	73–92	103–109	New Zealand	Poinar [76]

All data, with the exception of ratios and percentages, are given in micrometers, and are shown as the mean ± SD (range). Data for *H. casmirica* n. sp. are in italic. For abbreviations, see Table 1

[a] Dashes indicate that the data are not provided in the original publication

[b] Calculated from the drawings provided in the original publication

Bhat *et al. Parasites & Vectors* (2023) 16:383

Page 14 of 28

Table 3 Comparative morphometrics of *Heterorhabditis* adult males

Species	L	BD	EP	NR	NL	T	SL	GL	a	b	c	c'	SW%	GS%	D%
Heterorhabditis amazonensis	692–826	36–43	96–116	71–88	97–114	29–41	35–45	19–23	18.7[b]	7.7[c]	27.5[c]	1.3[c]	120–187	44–56	95–109
Heterorhabditis atacamensis	842–1025	42–55	116–149	69–93	99–119	24–36	40–49	17–22	19.7[b]	9.6[c]	29.3[c]	1.5[c]	179–249	38–51	108–126
Heterorhabditis bacteriophora	780–960	38–46	114–130	65–81	99–105	22–36	36–44	18–25	20.8[b]	9.1[b]	34.3[b]	1.8[b]	174	50	117
Heterorhabditis baujardi	818–970	45–53	71–93	54–77	105–132	28–38	33–45	18–22	16–22	6.4–8.8	24–33	1.5[c]	138–208	44–61	79[c]
Heterorhabditis beicherriana	889–1192	51–73	130–157	81–108	116–143	32–45	40–49	22–27	15–23	7.2–10	22–34	1.3–2.3	153–208	48–59	102–120
Heterorhabditis casmirica n. sp.	*608–914*	*24–48*	*102–120*	*58–80*	*100–118*	*16–32*	*38–48*	*18–26*	*15–24*	*6.4–8.2*	*24–35*	*1.1–1.6*	*160–252*	*45–63*	*99–107*
Heterorhabditis downesi	699–876	33–40	86–91	62–78	97–106	29–34	41–47	17–19	26.6[b]	8.8[c]	27.4[c]	1.4[c]	170–220	36–47	90
Heterorhabditis egyptii	594–848	31–56	80–97	56–84	96–109	23–34	25–50	16–22	17.1[b]	6.6[c]	19.5[c]	1.5[b]	120–220	40–65	84–91
Heterorhabditis floridensis	785–294	43–50	104–128	73–90	97–111	29–40	36–46	17–30	19.9[b]	7.9[c]	24.1[c]	1.4[c]	133–209	47–65	112
Heterorhabditis georgiana	721–913	43–55	101–145	72–93	100–122	29–41	41–49	20–28	16.5[b]	7.7[c]	26.1[c]	1.4[c]	150–200	51–64	100–122
Heterorhabditis hambletoni	510–800	38–60	80–100	80–90	–	–	–	–	–	–	–	–	–	–	–
Heterorhabditis indica	573–788	35–46	109–138	72–85	93–109	24–32	35–48	18–23	17.6[b]	6.7[c]	23.0[c]	1.1[c]	187	49	121
Heterorhabditis marelatus	805–1046	48–56	110–168	61–95	99–123	24–38	41–49	18–22	15.5[b]	7.8[c]	30.0[c]	1.1[c]	196	36–50	113[c]
Heterorhabditis megidis	800–1100	44–50	139–176	96–112	122–134	35–43	46–54	17–24	18–22	7–9	23–31	1.6[b]	188	43	122
Heterorhabditis mexicana	614–801	38–47	108–145	61–83	89–108	21–36	30–47	18–32	21.7[b]	6.8[c]	27.6[c]	1.1[c]	130–196	43–70	114–149
Heterorhabditis noenieputensis	530–775	34–46	75–102	64–75	88–106	21–32	37–49	17–24	14–18	5.6–7.9	21–33	1.1–1.7	202–301	38–56	81–108
Heterorhabditis ruandica	652–863	40–51	61–109	56–74	84–117	21–29	34–50	16–23	15–21	5.8–9.7	23–36	0.6–1.7	150–306	35–57	61–97
Heterorhabditis safricana	777–1009	40–58	104–147	52–61	105–126	27–49	35–54	19–27	20.1[b]	7.9[c]	43.0[c]	1.5[b]	130–259	43–62	92–133
Heterorhabditis taysearae	648–736	38–48	78–120	54–88	85–123	20–29	30–42	12–21	15.1[b]	6.5[c]	14.0[c]	1.3[c]	156	46	88
Heterorhabditis zacatecana	811–914	41–56	77–109	60–78	71–108	21–33	38–55	15–25	15–25	7.6–12	26–43	1.2–2.5	170–320	40–60	78–134
Heterorhabditis zealandica	848–1044	36–45	130–150	–	110–128	30–41	48–55	19–25	–	–	–	1.7[b]	246	44	118

All data, with the exception of ratios and percentages, are given in micrometers, and are shown as the mean ±SD (range). Data for *H. casmirica* n. sp. are in italic. For abbreviations, see Table 1

[a] Dashes indicate that the data are not provided in the original publication

[b] Calculated from the drawings provided in the original publication

[c] Calculated from other measurements provided in the original publication

Bhat *et al. Parasites & Vectors* (2023) 16:383

Page 15 of 28

Table 4 Comparative morphometrics of *Heterorhabditis* hermaphroditic females

Species	L	BD	EP	NR	NL	T	a	b	c	c'	V%	ABD	D%
Heterorhabditis amazonensis	3517–5587	220–316	184–238	128–171	180–225	104–154	–	–	–	2.3[b]	42–47	59–83	103[b]
Heterorhabditis atacamensis	1791–2904	88–122	165–206	101–132	174–200	72–112	–	–	–	2.7[b]	39–48	30–46	90–114
Heterorhabditis bacteriophora	3630–4390	160–180	189–217	121–130	189–205	81–93	–	–	–	–	41–47	40–53	106
Heterorhabditis baujardi	3135–4170	180–240	156–192	119–147	186–206	66–114	15–19	16–21	36–50	2.0[b]	43–48	47–63	88[b]
Heterorhabditis beicherriana	3671–5543	198–374	165–297	135–243	192–343	68–130	13–20	13–25	34–62	1.0–2.3	41–49	51–92	76–94
Heterorhabditis casmirica n. sp.	*2851–4219*	*140–341*	*180–211*	*77–100*	*174–207*	*72–114*	*19–27*	*16–39*	*56–84*	*1.4–2.2*	*46–57*	*36–56*	*94–120*
Heterorhabditis downesi	3030–5051	183–291	200–254	175–230	230–244	60–70	–	–	–	1.1[b]	50–55	57–65	117[b]
Heterorhabditis egyptii	2100–3100	107–164	154–205	101–147	144–192	83–115	–	–	–	2.7[b]	46–59	33–51	104[b]
Heterorhabditis floridensis	3731–5865	217–331	211–391	169–271	271–391	84–126	–	–	–	2.5[b]	44–49	42–78	104[b]
Heterorhabditis georgiana	3232–4928	157–267	200–277	143–217	132–271	65–96	–	–	–	1.2[b]	44–55	42.6[b]	–
Heterorhabditis hambletoni	–[a]	–	–	–	–	–	–	–	–	–	–	–	–
Heterorhabditis indica	2300–3100	107–145	163–187	104–123	163–179	72–110	–	–	–	–	45–50	38–51	–
Heterorhabditis marelatus	3000–4500	161–233	212–287	133–182	190–244	75–101	–	–	–	1.3[b]	45–50	20–28	109[b]
Heterorhabditis megidis	2400–4900	120–133	193–270	139–178	106–269	95–124	14–24	12–21	23–49	–	45–50	36–86	–
Heterorhabditis mexicana	2440–4606	135–267	103–201	114–171	168–221	94–170	–	–	–	2.6[b]	30–58	40–46	90[b]
Heterorhabditis noenieputensis	2987–5498	168–289	152–209	112–152	166–220	79–120	14–23	18–28	37–58	1.7–3.4	39–47	26–56	77–112
Heterorhabditis ruandica	2907–4123	209–274	106–153	78–108	134–159	63–98	12–16	21–27	34–51	1.7–2.6	45–55	29–51	67–103
Heterorhabditis safricana	3373–4073	127–188	210–267	121–163	199–236	64–91	–	–	–	–	43–46	40–54	98–119
Heterorhabditis taysearae	2200–2800	116–170	137–182	83–120	161–200	72–100	–	–	–	–	40–64	41–67	–
Heterorhabditis zacatecana	4408–6179	235–385	108–190	96–169	174–231	63–87	13–20	20–34	52–90	1.2–2.4	36–57	34–58	55–95
Heterorhabditis zealandica	–[a]	–	–	–	–	–	–	–	–	–	–	–	–

All data, with the exception of ratios and percentages, are given in micrometers, and are shown as the mean ± SD (range). Data for *H. casmirica* n. sp. are in italic. For abbreviations, see Table 1

[a] Dashes indicate that the data are not provided in the original publication

[b] Calculated from the drawings provided in the original publication

Table 5 Comparative morphometrics of *Heterorhabditis* amphimictic females

Species	L	BD	EP	NR	NL	T	a	b	c	c'	V	ABD	D%
Heterorhabditis amazonensis	1279–2070	70–122	103–126	68–100	119–142	25–38	–	–	–	2.4[b]	46–50	25–38	–
Heterorhabditis atacamensis	1754–2628	86–129	154–182	79–119	129–167	80–108	–	–	–	3.8[b]	43–49	24–33	100–113
Heterorhabditis bacteriophora	3180–3850	160–220	174–214	93–118	155–183	71–93	21.4[b]	18.8	41.5[b]	3.1[b]	42–53	22–31	114
Heterorhabditis baujardi	1335–2130	90–150	104–149	75–122	131–185	68–89	12–16	10–12	19–32	–	46–51	27–41	–
Heterorhabditis beicherriana	1581–3026	125–218	95–165	59–138	105–186	68–105	10–18	10–23	19–34	1.6–2.4	41–49	35–81	88–98
Heterorhabditis casmirica n. sp.	1273–1990	73–150	135–157	84–111	132–156	64–83	14–15	10–13	16–31	1.6–2.5	45–52	22–30	99–116
Heterorhabditis downesi	1231–2728	74–131	99–126	117–151	111–155	70–122	–	–	–	2.5[b]	47–60	25–38	–
Heterorhabditis egyptii	1050–1420	56–84	69–106	69–94	106–125	56–78	17.5[c]	14.4[c]	22.2[c]	3.1[c]	44–51	19–27	78[c]
Heterorhabditis floridensis	2054–2548	120–156	110–168	86–122	126–178	69–87	–	–	–	–	44–50	32–42	–
Heterorhabditis georgiana	1640–2779	101–188	111–177	96–162	136–219	62–88	–	–	–	1.5[b]	46–53	42[b]	–
Heterorhabditis hambletoni	600–1200	70–100	80–90	70–80	–	–	–	–	–	–	50–58[c]	–	–
Heterorhabditis indica	1200–1800	76–113	118–138	88–96	120–139	66–88	–	–	–	–	40–53	22–32	–
Heterorhabditis marelatus	1600–2600	113–177	139–178	79–119	129–164	55–81	–	–	–	1.3[b]	45–50	29–48	110[b]
Heterorhabditis megidis	1500–2500	95–140	158–206	105–120	155–168	70–101	15–19	10–16	18–32	2.6[b]	47–51	25–38	119[b]
Heterorhabditis mexicana	1144–2108	65–123	114–148	76–103	121–150	76–106	–	–	–	–	44–51	21–36	–
Heterorhabditis noenieputensis	1075–1697	76–129	102–125	73–90	115–132	63–75	13–17	9–14	17–24	2.3–3.1	40–53	22–32	83–104
Heterorhabditis ruandica	1131–1608	68–83	92–129	69–97	107–132	62–88	15–20	9.0–14	16–24	1.9–3.6	41–51	18–34	74–104
Heterorhabditis safricana	1679–2937	102–229	151–196	87–139	148–180	55–111	–	–	–	1.3[b]	45–50	25–72	97–120
Heterorhabditis taysearae	830–1400	42–96	120–166	76–109	129–179	62–80	–	–	–	4.0[b]	44–73	19–28	82[b]
Heterorhabditis zacatecana	1954–2798	160–228	100–133	71–96	112–148	45–75	11–15	16–21	31–63	1.3–2.0	43–61	31–41	80–111
Heterorhabditis zealandica	–[a]	–	–	–	–	–	–	–	–	–	–	–	–

All data, with the exception of ratios and percentages, are given in micrometers, and are shown as the mean ±SD (range). Data for *H. casmirica* n. sp. are in italic. For abbreviations, see Table 1

[a] Dashes indicate that the data are not provided in the original publication

[b] Calculated from the drawings provided in the original publication

[c] Calculated from other measurements provided in the original publication

Bhat *et al. Parasites & Vectors* (2023) 16:383

Page 17 of 28

conoid, surrounded by intestinal tissue. Rectum narrow and hardly visible. Anus closed. Tail conoid with refringent acute tip without mucron. Phasmids very small, located at posterior part of tail.

Diagnosis of *H. casmirica* n. sp.

Heterorhabditis casmirica n. sp. is characterized by having females and males with six conoid oral liplets, pore-like amphids and a robust pharynx, pharynx slender in juveniles, nerve ring surrounding the isthmus and excretory pore at basal bulb or intestine level in adults and at isthmus level in juveniles. Hermaphroditic females 2.8–4.2 mm long, with conoid tail (72–114 μm long, $c = 56$–84, $c' = 1.4$–2.2) with narrower tip; amphimictic females 1.2–2.0 mm long, with conoid tail (64–83 μm long, $c = 16$–31, $c' = 1.6$–2.5); males 0.6–0.9 mm long, with ventrally curved tail (16–32 μm long, $c = 24$–32, $c' = 1.1$–1.6), bursa with nine bursal papillae, spicules 38–48 μm long with manubrium with refractive walls, frequently smaller at the left spicule, gubernaculum 18–26 μm long with hook-like manubrium; juvenile with a tubular stoma and narrow and slender pharynx, second-stage juvenile (J2) 0.4–0.5 μm long, with cuticle with longitudinal ridges and conoid-elongate tail with finely rounded tip, and third-stage juvenile (J3) 0.5–0.6 μm long, with transversal annuli, a lateral field with two longitudinal ridges, oral opening with dorsal tooth and conoid tail with refringent acute tip.

Morphological relationships of *H. casmirica* n. sp. with other closely related species

Heterorhabditis casmirica n. sp. shares morphological similarities with *Heterorhabditis bacteriophora* [62], *Heterorhabditis beicherriana* [63], *Heterorhabditis egyptii* [18], *Heterorhabditis georgiana* [64], *Heterorhabditis ruandica* [17], and *Heterorhabditis zacatecana* [17]. However, several distinct morphological and morphometric characteristics can be used to differentiate *H. casmirica* n. sp. from these closely related species (Tables 2, 3, 4, 5).

IJs of *H. casmirica* n. sp. can be differentiated from those of *H. bacteriophora* by differences in the *c* ratio (4.7–6.4 vs. 5.7–7.0), the presence of a bacterial sac (invisible vs. visible in the ventricular portion of the intestine), and size of phasmids (very small at the posterior part of the tail vs. inconspicuous). Compared to *H. beicherriana* IJs, those of *H. casmirica* n. sp. differ in the shape of amphidial apertures (oval vs. inconspicuous), the position of the excretory pore (at isthmus level vs. at the beginning of the basal bulb), visibility of the bacterial sac (invisible vs. visible), and the size of phasmids (very small at the posterior part of the tail vs. inconspicuous). When compared to *H. egyptii*,

H. casmirica n. sp. differs in IJ tail length (85–115 vs. 53–75 μm), anterior end to excretory pore distance (98–129 vs. 81–94 μm), *c* ratio (4.7–6.4 vs. 6.8–9.1), and *D*% (83–97 vs. 74–82). When compared to *H. georgiana*, *H. casmirica* n. sp. IJs exhibit distinctions in visibility of the bacterial cell (invisible vs. visible posterior to cardia), with that in J2 and J3 occupying more than one half of the tail length (vs. about one half), and in phasmid size (very small at the posterior part of the tail vs. inconspicuous). When compared to *H. ruandica*, *H. casmirica* n. sp. IJs can be distinguished by the anterior end to nerve ring distance (79–94 vs. 52–64 μm), the position of the excretory pore (at isthmus level vs. at or just posterior to the basal bulb), tail length (85–115 vs. 49–64 μm), neck length (114–138 vs. 75–102 μm), *c* ratio (4.7–6.4 vs. 3.4–5.8), and presence of a cephalic tooth (small vs. large). When compared to *H. zacatecana*, the IJs of *H. casmirica* n. sp. differ in maximum body diameter (17–24 vs. 23–27 μm), the position of the excretory pore (at isthmus level vs. at or just posterior to the basal bulb), the anterior end to nerve ring distance (79–94 vs. 69–72 μm), neck length (114–138 vs. 78–99 μm), tail length (85–115 vs. 52–63 μm), *c* ratio (4.7–6.4 vs. 8.2–10), and *c'* ratio (5.1–8.0 vs. 4.3–6.7). A detailed comparison of the morphology of the IJs of *H. casmirica* n. sp. with those of other *Heterorhabditis* species is given in Table 2.

The males of *H. casmirica* n. sp. can be distinguished from those of *H. bacteriophora* based on the neck length (106–118 vs. 99–105 μm), *b* ratio (6.4–8.2 vs. 9.1), *c'* ratio (1.1–1.6 vs. 1.8), *D*% (99–107 vs 117 μm), spicules with a rectangular manubrium with strongly refringent walls (vs rectangular with scarcely refringent walls), gubernaculum more than a half of the spicule length (vs. shorter) and GP1 at the level of the manubrium (vs. more anterior in the type population). In comparison to male *H. beicherriana*, differences include body size (0.6–0.9 vs. 0.9–1.2 mm), maximum body diameter (24–48 vs. 51–73 μm), the distance from the anterior end to the excretory pore (102–120 vs. 130–157 μm), the distance from the anterior end to the nerve ring (58–80 vs. 81–108 μm), the tail length (16–32 vs. 32–45 μm), *D*% (99–107 vs. 102–120 μm), GP1 at spicule level (vs. more anterior), the shape of the spicule manubrium (quadrangular vs. oblongate) and gubernaculum (more than half of the spicule length vs. similar length). Compared to males of *H. egyptii*, differences lie in the *c* ratio (24–35 vs. 19.5). When compared to males of *H. georgiana*, differences lie in the position of the excretory pore (at bulb or intestine level vs. posterior to the basal bulb only), spicules with rectangular manubrium with strongly refringent walls (vs rectangular with scarcely refringent walls) and gubernaculum (more than a half of the spicule length vs. a half

Bhat *et al. Parasites & Vectors* (2023) 16:383

Page 18 of 28

of the spicule length). Compared to males of *H. ruandica*, differences include the shape of the spicule manubrium (well developed, quadrangular and with strongly refringent walls vs. poorly developed, triangular and not refringent), the shape of the gubernaculum manubrium (hook-like vs. straight) and gubernaculum (more than a half of the spicule length vs. a half). Compared to males of *H. zacatecana*, differences include the shape of the spicule manubrium (quadrangular with strongly refringent walls vs. rounded and not refringent), bursa with GP1-GP2 distance shorter (less than the corresponding body diameter vs. slightly longer), GP2–GP3 slightly separated (vs. very closed), spicule manubrium (with angular anterior end vs. with rounded anterior end), the shape of the gubernaculum manubrium (hook-like vs. slightly curved) and gubernaculum more than a half of the spicule length (vs. shorter). Lastly, differences from males of *H. hambletoni* include the distance from the anterior end to the nerve ring (58–80 vs. 80–90 μm). With respect to the males of all of the other species, *H. casmirica* n. sp. has a different spicule morphology (manubrium with thick and refringent walls and lacking a dorsal hump vs. thin walls and a small dorsal hump) and gubernaculum with a hook-like manubrium (vs. straight).

The hermaphroditic females of *H. casmirica* n. sp. can be distinguished from those of *H. bacteriophora* based on several characteristics, including the distance from the anterior end to the nerve ring (77–100 vs. 121–130 μm), and a larger *V*% (46–57 vs. 41–47). The hermaphroditic females of the new species can be differentiated from those of *H. beicherriana* by the distance from the anterior end to the nerve ring (77–100 vs. 135–243 μm), and a smaller anal body diameter (36–56 vs. 51–92 μm). Additionally, hermaphroditic females of *H. casmirica* n. sp. differ from those of *H. egyptii* by the distance from the anterior end to the nerve ring (77–100 vs. 101–147 μm); from those of *H. georgiana* by the distance from the anterior end to the excretory pore (180–211 vs. 200–277 μm) and the distance from the anterior end to the nerve ring (77–100 vs. 143–217 μm); from those of *H. ruandica* in tail shape (conoid vs. conoid-elongate) and size (longer vs. short), visible uteri (vs. not well visible), the *a* ratio (19–27 vs. 12–16), and *c* ratio (56–84 vs. 34–51); from those of *H. zacatecana* by shorter length (0.28–0.42 vs. 0.44–0.62 mm), the distance from the anterior end to the nerve ring (77–100 vs. 96–169 μm), visible oviducts and uteri (vs. not well visible), and shorter neck length (154–176 vs. 174–231 μm).

Amphimictic females of *H. casmirica* n. sp. can be differentiated from those of *H. bacteriophora* by their shorter rectum (slightly longer than the anal body diameter vs. about three times longer in the type population), smaller phasmids (vs. inconspicuous), shorter length (0.13–2.0 vs. 0.32–0.39 mm), smaller maximum body diameter (73–150 vs. 160–220 μm), the distance from the anterior end to the excretory pore (135–157 vs. 174–214 μm), and demanian ratios. Compared to *H. beicherriana*, amphimictic females of *H. casmirica* n. sp. have a shorter tail (conoid vs. conoid-elongate), with an acute tip (vs. finely rounded tip), differ in their phasmids (very small vs. inconspicuous), and have a smaller anal body diameter (22–30 vs. 35–81 μm). In comparison to *H. egyptii*, amphimictic females of *H. casmirica* n. sp. have a shorter tail (conoid vs. conoid-elongate), longer distance from the anterior end to the excretory pore (135–157 vs. 69–106 μm), and longer neck length (132–156 vs. 106–125 μm). Additionally, amphimictic females of *H. casmirica* n. sp. differ from those of *H. georgiana* by having smaller phasmids (vs. inconspicuous), and from those of *H. ruandica* by having a longer neck (132–156 vs. 107–132 μm), different *a* ratio (14–15 vs. 15–20), and smaller phasmids (vs. inconspicuous). Finally, compared to amphimictic females of *H. zacatecana*, those of the new species have a smaller maximum body diameter (73–150 vs. 160–228 μm), different *b* ratio (10–13 vs. 16–21), *c* ratio (16–31 vs. 31–63), smaller phasmids (vs. inconspicuous), and smaller anal body diameter (22–30 vs. 31–41 μm). Summaries of the similarities and differences between males, hermaphroditic females, and amphimictic females of *H. casmirica* n. sp. and other *Heterorhabditis* species are presented in Tables 3, 4, 5, respectively.

Life cycle

Heterorhabditis casmirica n. sp. is a highly pathogenic nematode species that can be easily raised on *G. mellonella* larvae at a temperature ranging from 18 to 24 °C. The life cycle of this new species is comparable to that of other *Heterorhabditis* species. When *G. mellonella* larvae are exposed to 50–100 IJs, they die within 36–48 h and appear bright reddish after 48–72 h. First- and second-generation adults of *H. casmirica* n. sp. can be found in the insect cadavers 5–6 and 7–9 days after infection, respectively. The pre-infective juveniles left the host body, matured for a few days, and then migrated to the water traps after 15–21 days.

Type host and locality

The specific host for *H. casmirica* n. sp. is currently unknown as these nematodes were isolated from soil samples using the insect baiting technique [24, 77, 78]. *Heterorhabditis casmirica* n. sp. populations were collected from soil samples in the union territory of Jammu and Kashmir, located in the northwest region of India, and specifically in the Himalayan Pir Panjal region.

Bhat *et al. Parasites & Vectors* (2023) 16:383

Page 19 of 28

Type material

The type material for *H. casmirica* n. sp. (holotype male, 15 hermaphroditic female paratypes, 15 male paratypes, 15 amphimictic female paratypes and 19 J3, all belonging to the HM population) were deposited in the National Nematode Collection of India, Indian Agricultural Research Institute, New Delhi. Nematode cultures are maintained at the Sher-e-Kashmir University of Agricultural Sciences and Technology of Kashmir, India.

Etymology

The specific name "*casmirica*" is derived from the Kashmir division (Casmiria in Latin), the geographical region where the nematodes used to describe the new species were collected.

Cross-hybridization experiments

No viable offspring were observed when *H. casmirica* n. sp. nematodes of the HM strain were allowed to interact with Indian populations of *H. bacteriophora*, *H. indica*, and *H. baujardi*. However, fertile progenies were observed when six different populations of *H. casmirica* n. sp. nematodes were allowed to interact, indicating that these populations are conspecific but reproductively isolated from closely related species, including *H. bacteriophora*, *H. indica*, and *H. baujardi*. Fertile progeny was also observed when all the nematode strains self-fertilized.

Nematode molecular characterization

The six populations of *H. casmirica* n. sp. were molecularly characterized based on the sequences of various genetic regions, including the ITS region of the rRNA (NCBI accession numbers OQ517936–OQ517941), the D2–D3 expansion segments of 28S rRNA (NCBI accession numbers OQ517947–OQ517952), mitochondrial 12S rRNA (NCBI accession numbers OQ517975-OQ517980), and *MT-COI* (NCBI accession numbers OQ517969–OQ517974). The ITS region of *H. casmirica* n. sp. is 771 bp in length, with ITS1 comprising 389 bp, 5.8S comprising 154 bp, and ITS2 comprising 228 bp. The *MT-COI* region flanked by primers HCF and HCR of *H. casmirica* n. sp. shows sequence similarity scores ranging from 75 to 94% with other *Heterorhabditis* species, and differs in 17–57 nucleotide positions (Table 6). Considering this genetic region, *H. casmirica* n. sp. is closely related to *H. bacteriophora*, *H. ruandica*, and *H. zacatecana* (Table 6). *Heterorhabditis bacteriophora* and *H. ruandica* both share 94% similarity with *H. casmirica* n. sp. and differ in 17 nucleotide positions. *Heterorhabditis zacatecana* shares 93% similarity with *H. casmirica* n. sp., and differs in 21 nucleotide positions. Fewer differences between *H. casmirica* n. sp. and its more closely related

species were observed in the rRNA gene sequences. When compared with *H. casmirica* n. sp., *H. bacteriophora* and *H. zacatecana* both share 99.7% similarity and differ in two nucleotide positions, while *H. ruandica* shares 99.5% similarity and differs in four nucleotide positions in the ITS rRNA sequences flanked by primers TW81 and AB28 (Additional file 1: Table S2). All these three species share 100% similarity in the D2–D3 rRNA sequences flanked by primers D2A and D3B (Additional file 1: Table S3). Currently, very few mitochondrial 12S rRNA gene sequences are publicly available for molecular comparisons and phylogenetic analysis. Nevertheless, the sequences obtained in this study were deposited in the NCBI database for future taxonomic studies.

Nematode phylogenetic reconstructions

Phylogenetic analyses based on different genetic markers show that *H. casmirica* n. sp. belongs to the "bacteriophora" clade, which is currently composed of *H. bacteriophora*, *H. beicherriana*, *H. georgiana*, *H. ruandica*, and *H. zacatecana* (Figs. 7, 8, 9). *MT-COI* is particularly useful for the differentiation of all of these closely related species, and clearly shows that *H. casmirica* n. sp. and *H. bacteriophora*, its more closely related species, form two independent subclusters (Fig. 7). However, sequences of the ITS and D2–D3 regions of the rRNA gene, although allowing for the differentiation of certain species (Figs. 7, 8), provide lower phylogenetic resolving power than the *MT-COI* gene, as reported by Dhakal et al. [46] and Machado et al. [17]. Hence, *MT-COI* is particularly useful for the molecular discrimination of closely related species of the genus *Heterorhabditis*.

Morphological and molecular relationships between *H. casmirica* n. sp. and specimens of *H. bacteriophora* present in India

At the morphological level, *H. casmirica* n. sp. differs from previously reported Indian isolates of *H. bacteriophora* [22, 30] (Additional file 1: Table S1). In particular, we observed that the males differ in spicule manubrium with strongly refringent walls (vs with scarcely refringent walls), gubernaculum more than a half of the spicule length (vs. shorter) and GP1 at manubrium level (vs. more anterior in the type population). The amphimictic females differ in smaller phasmids (vs. inconspicuous). The IJs differ in the distance from the anterior end to the nerve ring (79–94 vs. 48–74 µm), presence of bacterial sac (invisible vs. visible in the ventricular portion of the intestine), and size of phasmids (very small at posterior part of tail vs. inconspicuous) (Additional file 1: Table S1).

At the molecular level, *H. casmirica* n. sp. differs in 17 nucleotide positions in the *MT-COI* gene from several

Bhat *et al. Parasites & Vectors* (2023) 16:383

Page 20 of 28

Table 6 Pairwise distances (in base pairs) of the mitochondrially encoded cytochrome C oxidase subunit I gene (*MT-COI*) regions between *Heterorhabditis casmirica* n. sp and other species of *Heterorhabditis*

Species (MT-COI)	*Heterorhabditis casmirica* n. sp. (HM population)	*Heterorhabditis bacteriophora* TT01	*Heterorhabditis ruandica* Rwl4_N-C4a	*Heterorhabditis zacatecana* MEX-39	*Heterorhabditis beicheriana* CD2516	*Heterorhabditis georgiana* CD2500	*Heterorhabditis zealandica* CD2507	*Heterorhabditis megidis* CD2518	*Heterorhabditis atacamensis* MEX-20	*Heterorhabditis marelatus*	*Heterorhabditis downesi* CD2508	*Heterorhabditis mexicana*	*Heterorhabditis floridensis* CD2503	*Heterorhabditis tayserae*	*Heterorhabditis amazonensis* CD2510	*Heterorhabditis baujardi* CD2519	*Heterorhabditis noenieputensis* CD2506	*Heterorhabditis indica* LN2
Heterorhabditis casmirica n. sp. (HM population)		*17*	*18*	*21*	*23*	*27*	*30*	*35*	*42*	*42*	*42*	*44*	*45*	*45*	*46*	*47*	*52*	*57*
Heterorhabditis bacteriophora TT01	*94*		19	19	21	23	31	32	42	40	35	36	41	37	41	39	44	50
Heterorhabditis ruandica Rwl4_N-C4a	*94*	94		8	16	24	32	29	40	36	31	45	48	45	49	45	51	55
Heterorhabditis zacatecana MEX-39	*93*	94	98		21	24	31	31	41	37	32	44	47	46	48	46	51	54
Heterorhabditis beicheriana CD2516	*92*	93	95	93		22	26	27	36	30	31	44	44	42	47	41	48	49
Heterorhabditis georgiana CD2500	*91*	92	92	92	93		29	23	33	32	26	40	43	42	38	37	50	47
Heterorhabditis zealandica CD2507	*89*	89	89	89	91	90		24	34	30	34	39	40	42	41	35	46	46
Heterorhabditis megidis CD2518	*87*	89	90	89	91	92	92		33	28	21	39	41	42	42	35	52	41
Heterorhabditis atacamensis MEX-20	*84*	84	85	85	87	88	88	88		26	37	47	49	47	43	38	46	47
Heterorhabditis marelatus	*84*	85	87	86	89	89	89	90	91		34	45	48	48	47	42	50	48
Heterorhabditis downesi CD2508	*84*	87	89	89	89	91	88	93	86	88		41	41	42	42	35	53	47
Heterorhabditis mexicana	*83*	87	82	83	82	84	85	85	82	82	84		11	13	26	19	45	45
Heterorhabditis floridensis CD2503	*82*	84	81	82	82	83	85	84	81	81	83	97		18	33	26	47	43
Heterorhabditis tayserae	*82*	86	82	82	83	83	84	84	82	81	83	96	94		31	20	44	50
Heterorhabditis amazonensis CD2510	*82*	84	80	81	81	85	84	84	84	81	83	91	88	89		27	48	49
Heterorhabditis baujardi CD2519	*81*	85	83	82	84	86	87	87	86	84	87	94	91	94	91		45	40
Heterorhabditis noenieputensis CD2506	*77*	82	78	78	80	79	80	77	81	79	76	82	81	82	80	82		37
Heterorhabditis indica LN2	*75*	79	76	77	79	81	81	84	81	80	81	82	83	80	80	85	86	

Data for *H. casmirica* n. sp. are in italic. . Data below the diagonal indicate percentage similarity. Data above the diagonal indicate the total difference between the characters

Bhat *et al. Parasites & Vectors* (2023) 16:383
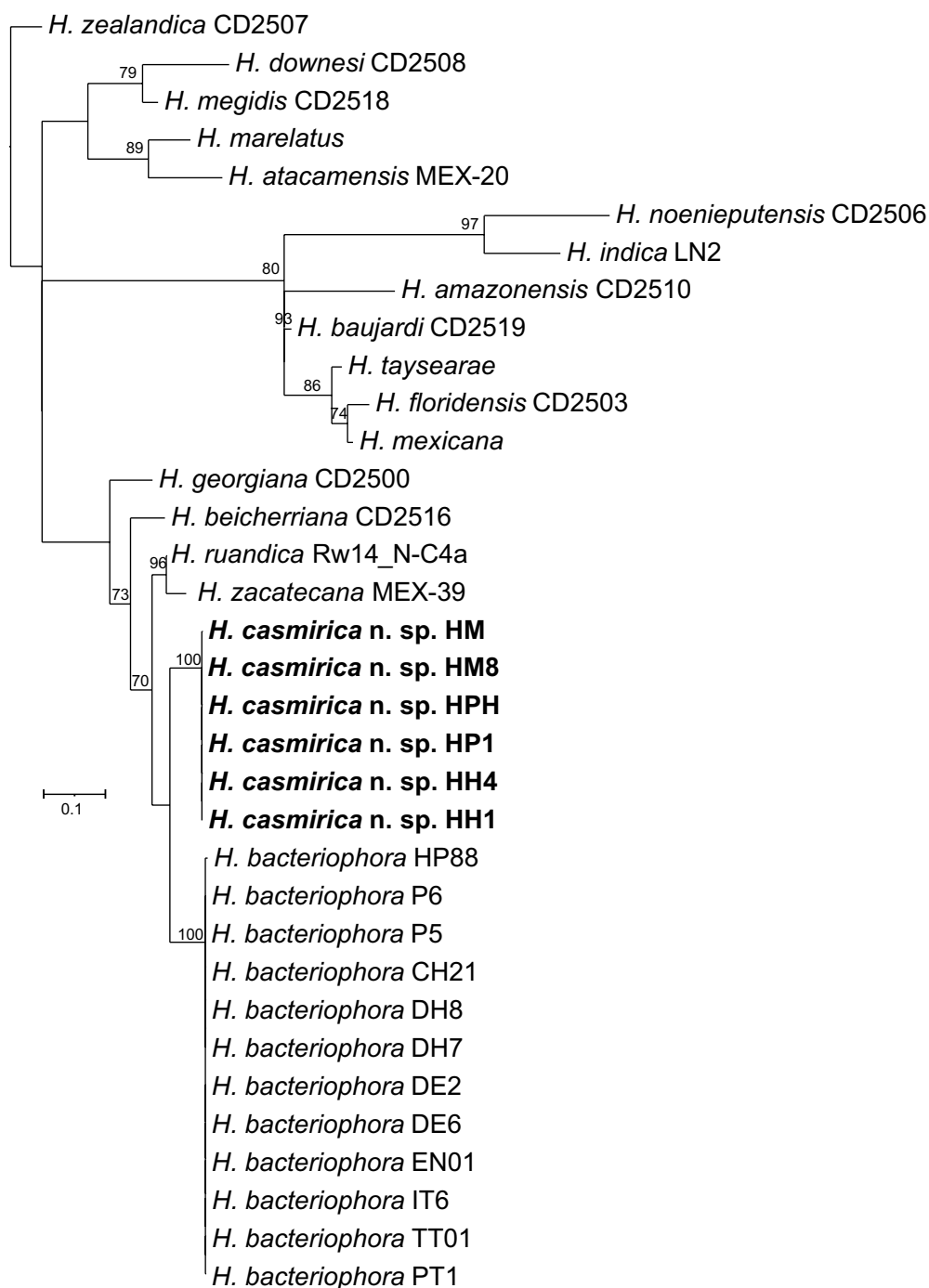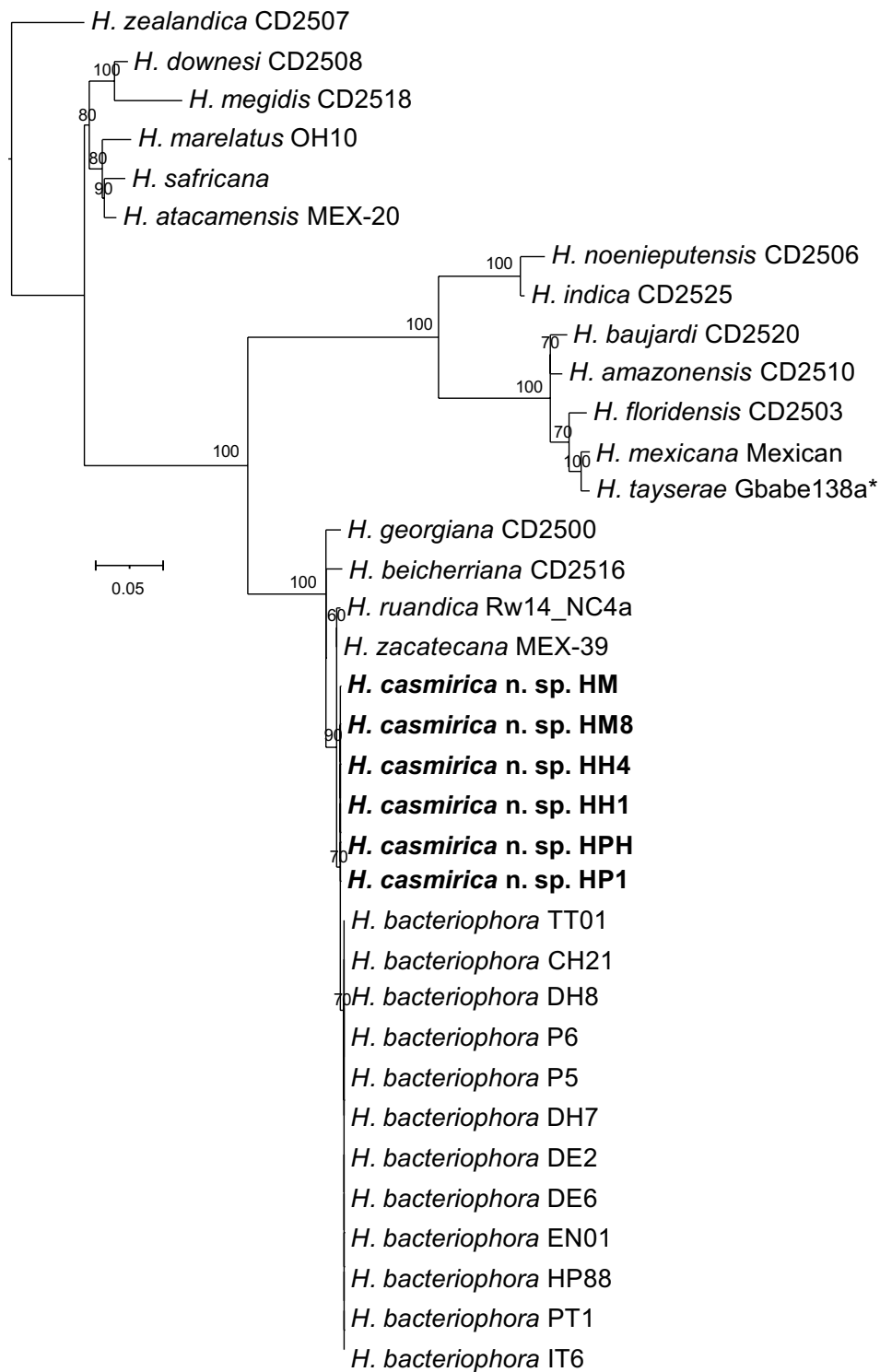
Page 21 of 28

Fig. 7 Maximum-likelihood phylogenetic tree between the newly described *Heterorhabditis casmirica* n. sp. and described species of *Heterorhabditis* based on nucleotide sequences of *MT-COI* flanked by primers HCF and HCR. Numbers at nodes represent bootstrap values based on 100 replications. Bars represent average nucleotide substitutions per sequence position. Nation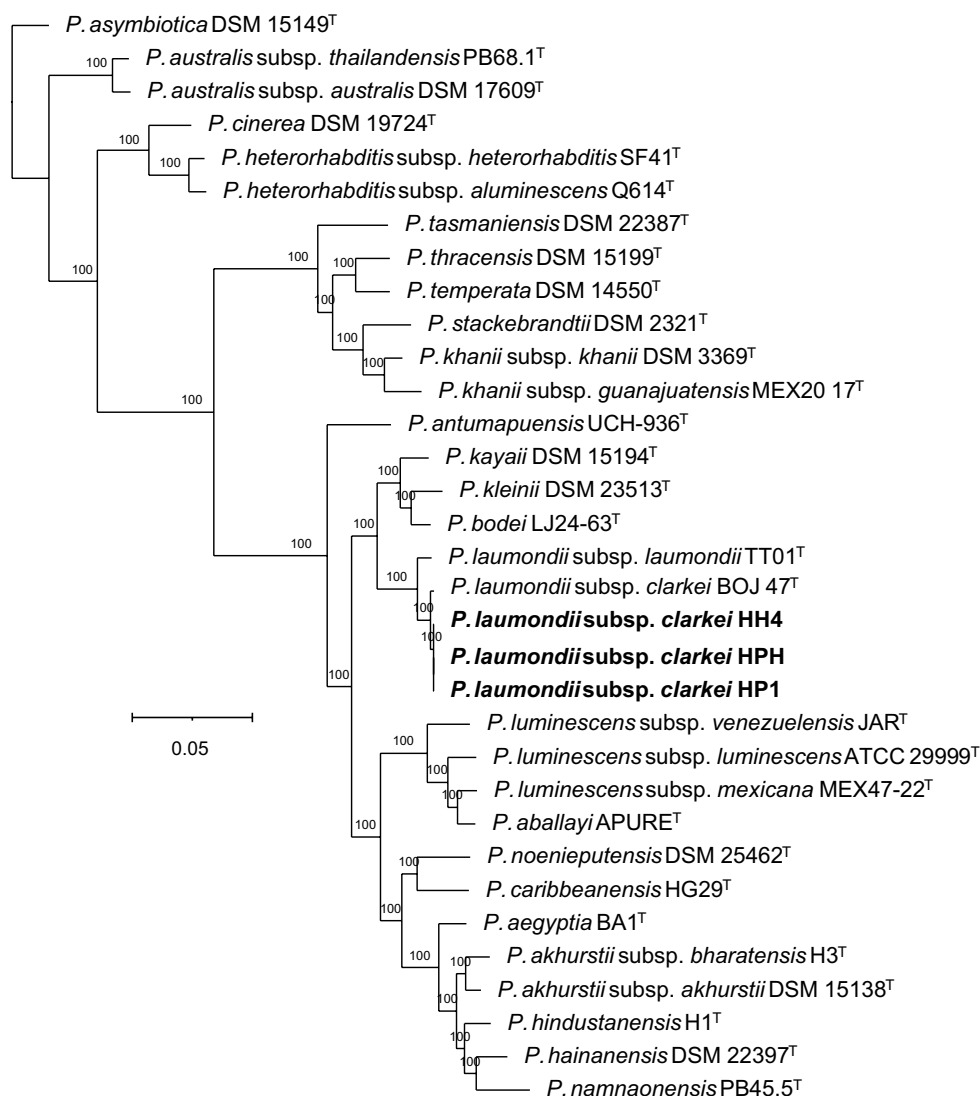al Center for Biotechnology Information (NCBI) accession numbers of the nucleotide sequences used for the analyses are shown in Additional file 1: Table S4. The scale bar shows the number of substitutions per site

H. bacteriophora isolates from India, such as DH7, DH8, CH21, P5 and P6. On average, *H. casmirica* n. sp. shares 94% similarity with these isolates. In addition, the Indian populations of *H. bacteriophora* share 99.7% similarity with *H. casmirica* n. sp., and differ in two nucleotide positions in the ITS rRNA gene. Lastly, these two species

Bhat *et al. Parasites & Vectors* (2023) 16:383

Page 22 of 28

Fig. 8 Maximum-likelihood phylogenetic tree between the newly described *Heterorhabditis casmirica* n. sp. and described species of *Heterorhabditis* based on nucleotide sequences of the internal transcribed spacer (ITS) (ITS1-5.8S-ITS2) ribosomal RNA (rRNA), flanked by primers 18S and 26S. Numbers at nodes represent bootstrap values based on 100 replications. Bars represent average nucleotide substitutions per sequence position. NCBI accession numbers of the nucleotide sequences used for the analyses are shown in Additional file 1: Table S4. The scale bar shows the number of substitutions per site

Bhat *et al. Parasites & Vectors* (2023) 16:383

Page 23 of 28
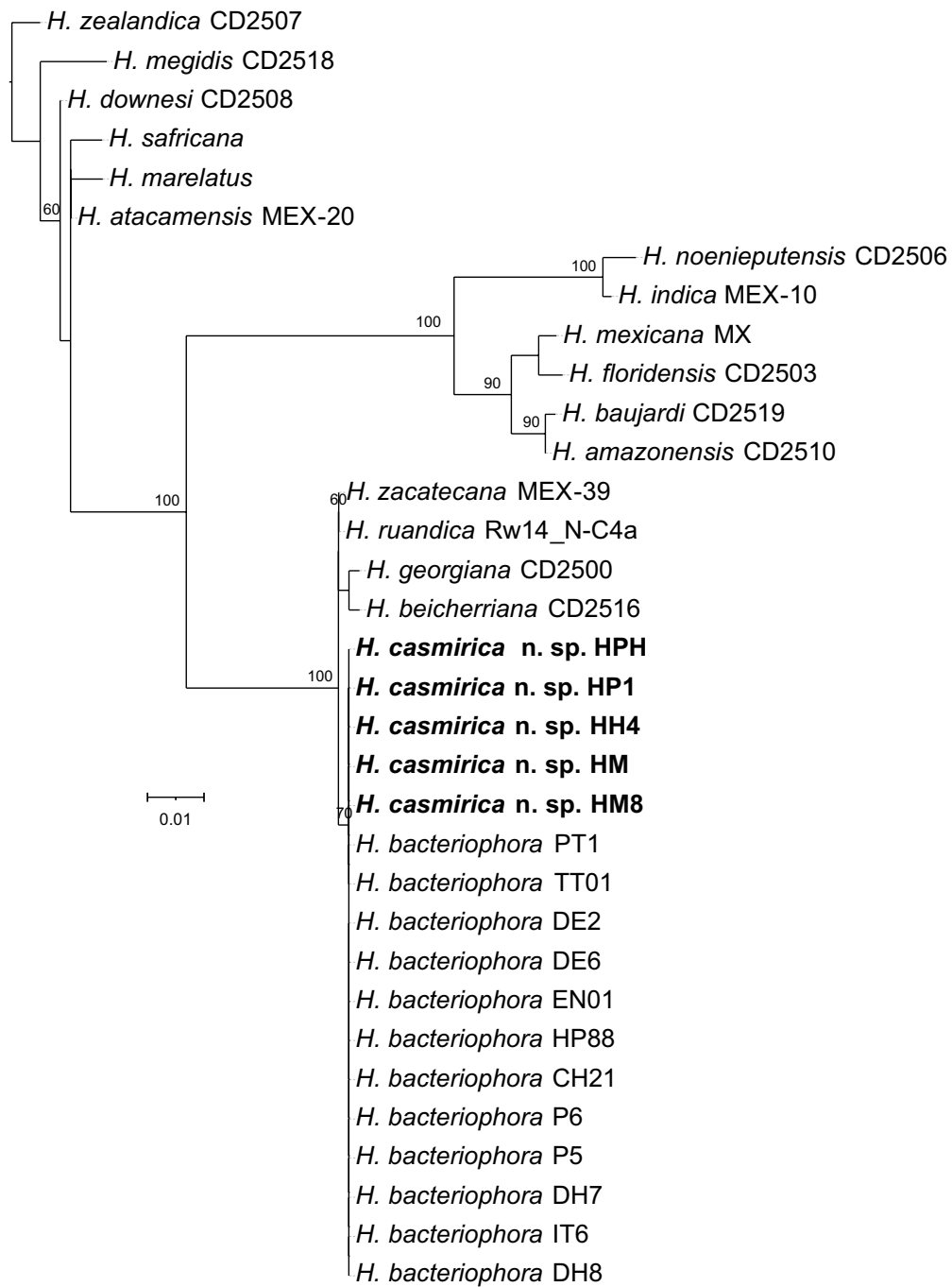
Fig. 9 Maximum-likelihood phylogenetic tree reconstructed from the nucleotide sequences of the D2–D3 expansion segments of the 28S rRNA (D2–D3), flanked by primers D2A and D2B. Accession numbers of the nucleotide sequences used for the analyses are shown in Additional file 1: Table S4. Numbers at nodes represent bootstrap values based on 100 replications. Bars represent average nucleotide substitutions per sequence position

Bhat *et al. Parasites & Vectors* (2023) 16:383

Page 24 of 28

Fig. 10 Phylogenetic reconstruction based on core genome sequences of *Photorhabdus* bacterial strains; 2,227,040 nucleotide positions (2216 core genes) were used in the analysis. Numbers at the nodes represent Shimodaira–Hasegawa-like branch supports. Bar represents average nucleotide substitutions per sequence position. NCBI accession numbers of the genome sequences used for the reconstruction are shown in Additional file 1: Table S5. The scale bar shows the number of substitutions per site

do not differ in the sequences of the D2–D3 rRNA gene. Notably, the Indian populations DH7, DH8, CH21, P5 and P6 share 100% similarity with the type population of *H. bacteriophora* across all the gene markers used, and hence corroborate the conclusions of previous studies [22, 30]. The phylogenetic study further confirms the distinctiveness of the Indian populations of *H. bacteriophora* from *H. casmirica* n. sp. and establishes their similitude with the type population of *H. bacteriophora* (Figs. 7, 8, 9).

Symbiotic relationships

Phylogenetic reconstructions based on core genome sequences and sequence comparisons show that the bacterial symbionts isolated from *H. casmirica* n. sp. are very similar and belong to the subspecies *Photorhabdus laumondii* subsp. *clarkei* (Fig. 10). The digital DNA–DNA hybridization (dDDH) scores between BOJ47[T], the type strain of the species *P. laumondii* subsp. *clarkei*, and strains HH4, HPH, and HP1, isolated from *H. casmirica*

Bhat *et al. Parasites & Vectors* (2023) 16:383

Page 25 of 28

n. sp. HH4, HPH and HP1, are 94.3%, which is above the 70 and 79% thresholds that delimit prokaryotic species and subspecies, and confirms that they are conspecific [79].

A side note on the nomenclature of *Heterorhabditis marelatus*

The term "*marelatus*" was created by combining the Latin words "*mare*" meaning sea and "*latus*" meaning side in an attempt to translate the type locality "seaside" into Latin [70]. Hence, *marelatus* was formed as a noun, not as an adjective. Sudhaus [80] changed the specific epithet of the species *Heterorhabditis marelatus* to "*marelata*." This change was perhaps motivated by the fact that the genus noun *Heterorhabditis* is feminine and that, in Latin, the specific epithet should agree in gender with the genus. However, nouns in Latin do not vary according to gender, and therefore we propose that the correct term is "*marelatus*." Hence, we propose that the original species nomenclature, *Heterorhabditis marelatus*, should be maintained.

Conclusions

Six populations of *Heterorhabditis* nematodes were identified in the present study that exhibited clear distinctions in their morphology, morphometric and molecular characteristics, as well as reproductive isolation and phylogenetic separation from all known *Heterorhabditis* species. We propose the name *Heterorhabditis casmirica* n. sp. for this new species, which is the second new *Heterorhabditis* entomopathogenic nematode species reported from the Indian subcontinent. Our results highlight the importance of using both classical taxonomy and molecular markers (*MT-COI*, ITS, small subunit, and large subunit) to accurately describe new *Heterorhabditis* species and their bacterial symbionts. The discovery of *H. casmirica* n. sp. and its associated bacterial symbiont expands our understanding of the biodiversity and distribution of these biocontrol agents and underscores their potential in the development of new biocontrol strategies against insect pests.

Abbreviations

GP	Genital papilla
IJs	Infective juveniles
ITS	Internal transcribed spacer
LB	Luria—Bertani
LM	Light microscopy
MT-COI	Mitochondrially encoded cytochrome C oxidase subunit I
NCBI	National Center for Biotechnology Information
SEM	Scanning electron microscopy

Supplementary Information

The online version contains supplementary material available at https://doi.org/10.1186/s13071-023-05990-z.

Additional file 1: Table S1. Comparative morphometrics of infective juveniles and adult generations of *Heterorhabditis casmirica* n. sp. with type populations of *Heterorhabditis bacteriophora* and Indian strains. All data, with the exception of ratios and percentages, are given in micrometers and as mean (range). **Table S2.** Pairwise distances in base pairs of the ITS rRNA regions between species of *Heterorhabditis* and *Heterorhabditis casmirica* n. sp. Data for *H. casmirica* n. sp. are in italic. **Table S3.** Pairwise distances in base pairs of the D2–D3 rRNA regions between species of *Heterorhabditis* and *Heterorhabditis casmirica* n. sp. Data for *H. casmirica* n. sp. are in italic. **Table S4.** National Center for Biotechnology Information (NCBI) accession numbers of the nucleotide sequences used for the phylogenetic analyses in this study; the sequences newly generated in this study are in italic. **Table S5.** NCBI accession numbers of the genomic sequences of different *Photorhabdus* species used in this study; the sequences newly generated in this study are in italic.

Availability of data and materials

Our sequences were deposited in the GenBank database under the accession numbers given in Additional file 1: Tables S3 and S4. Data supporting the conclusions of this article are included within the article. The datasets used and/or analyzed during the current study are available from the corresponding author upon reasonable request.

Declarations

Ethics approval and consent to participate

Not applicable.

Consent for publication

Not applicable.

Competing interests

The authors declare no conflict of interest exists.

Bhat *et al. Parasites & Vectors* (2023) 16:383

Page 26 of 28

Author details
¹Department of Biosciences, University Center for Research and Development, Chandigarh University, Gharuan, Mohali, Punjab 140413, India. ²Experimental Biology Research Group, Institute of Biology, Faculty of Sciences, University of Neuchâtel, Neuchâtel, 2000, Switzerland. ³Departamento de Biología Animal, Biología Vegetal y Ecología, Universidad de Jaén, Campus 'Las Lagunillas', Jaén, 23071, Spain. ⁴Division of Entomology, Faculty of Agriculture, Sher-e-Kashmir University of Agricultural Sciences and Technology of Kashmir, Wadura Campus, Sopore, 193201, Jammu and Kashmir, India. ⁵Department of Botany and Microbiology, College of Science, King Saud University, 11451 Riyadh, Saudi Arabia. ⁶Department of Zoology, University of Kashmir, Srinagar 190006, Jammu and Kashmir, India.

References
1. Clarke DJ. *Photorhabdus*: a tale of contrasting interactions. Microbiology. 2020;166:335–48.
2. Kajol Y, Bhat AH, Chaubey AK. Biochemical and molecular characterization of *Photorhabdus akhurstii* associated with *Heterorhabditis indica* from Meerut, India. Pak J Nematol. 2020;38:15–24.
3. Machado RAR, Bhat AH, Castaneda-Alvarez C, Půža V, San-Blas E. *Photorhabddus aballayi* sp. nov. and *P. luminescens* subsp. *venezuelensis* subsp. nov., isolated from *Heterorhabditis amazonensis* entomopathogenic nematodes. Int J Syst Evol Microbiol. 2023. https://doi.org/10.1099/ijsem.0.005872.
4. Bhat AH, Machado RAR, Abolafia J, Askary TH, Půža V, Ruiz-Cuenca AN, et al. Multigene sequence based and phenotypic characterization reveals the occurrence of a novel entomopathogenic nematode species, *Steinernema anantnagense* n. sp. J Nematol. 2023;55:e2023–31. https://doi.org/10.2478/jofnem-2023-0029.
5. Lefoulon E, McMullen JG, Stock SP. Transcriptomic analysis of *Steinernema* nematodes highlights metabolic costs associated to *Xenorhabdus* endosymbiont association and rearing conditions. Front Physiol. 2022;13:821845. https://doi.org/10.3389/fphys.2022.821845.
6. Ciche TA, Ensign JC. For the insect pathogen *Photorhabdus luminescens*, which end of a nematode is out? Appl Environ Microbiol. 2003;69:1890–7.
7. Hallem EA, Rengarajan M, Ciche TA, Sternberg PW. Nematodes, bacteria, and flies: a tripartite model for nematode parasitism. Curr Biol. 2007;17:898–904.
8. Bai X, Adams BJ, Ciche TA, Clifton S, Gaugler R, Kim K, et al. A lover and a fighter: the genome sequence of an entomopathogenic nematode *Heterorhabditis bacteriophora*. PLoS ONE. 2013;8:e69618. https://doi.org/10.1371/journal.pone.0069618.
9. RH Ffrench-Constant, Dowling A, Waterfield NR. Insecticidal toxins from *Photorhabdus* bacteria and their potential use in agriculture. Toxicon. 2007;49:436–51.
10. Rodou A, Ankrah DO, Stathopoulos C. Toxins and secretion systems of *Photorhabdus luminescens*. Toxins. 2020;2:1250–64.
11. Adams BJ, Fodor A, Koppenhofer HS, Stackebrandt E, Stock SP, Klein MG. Biodiversity and systematics of nematode-bacterium entomopathogens. Biol Control. 2006;37:32–49.
12. Mitani DK, Kaya HK, Goodrich-Blair H. Comparative study of the entomopathogenic nematode, *Steinernema carpocapsae*, reared on mutant and wild-type *Xenorhabdus nematophila*. Biol Control. 2004;29:382–91.
13. Ciche TA, Kim K, Kaufmann-Daszczuk B, Nguyen KCQ, Hall DH. Cell invasion and matricide during *Photorhabdus luminescens* transmission by *Heterorhabditis bacteriophora* nematodes. Appl Environ Microbiol. 2008;74:2275–87.
14. Ebssa L, Borgemeister C, Poehling HM. Effectiveness of different species/strains of entomopathogenic nematodes for control of western flower thrips (*Frankliniella occidentalis*) at various concentrations, host densities, and temperatures. Biol Control. 2004;29:145–54.
15. Bhat AH, Chaubey AK, Askary TH. Global distribution of entomopathogenic nematode, *Steinernema* and *Heterorhabditis*. Egypt J Biol Pest Control. 2020;30:31.
16. Hunt DJ, Subbotin SA. Taxonomy and systematics. In: Hunt DJ, Nguyen KB, editors. Advances in entomopathogenic nematode taxonomy and phylogeny. Nematol Monogr Perspect, vol. 12. Brill; 2016. p. 13–58.
17. Machado RAR, Bhat AH, Abolafia J, Muller A, Bruno P, Fallet P, et al. Multi-locus phylogenetic analyses uncover species boundaries and reveal the occurrence of two new entomopathogenic nematode species, *Heterorhabditis ruandica* n. sp. and *Heterorhabditis zacatecana* n. sp. J Nematol. 2021;53:e2021–89.
18. Abd-Elgawad MMM, Ameen HH. *Heterorhabditis egyptii* n. sp. (Rhabditida: Heterorhabditidae) from Egypt. Egypt J Agric Res. 2005;2:855–70.
19. Pereira C. *Rhabditis hambletoni* n. sp. nema apparentemente semiparasito da "broca do algodoeiro" (*Gasterocercodes brasiliensis*). Arch Inst Biol. 1937;8:215–30.
20. Poinar GO, Karunakar GK, David H. *Heterorhabditis indicus* n. sp. (Rhabditida: Nematoda) from India: separation of *Heterorhabditis* spp. by infective juveniles. Fund Appl Nematol. 1992;15:467–72.
21. Bhat AH, Chaubey AK, Shokoohi E, Machado RAR. Molecular and phenotypic characterization of *Heterorhabditis indica* (Nematoda: Rhabditida) nematodes isolated during a survey of agricultural soils in western Uttar Pradesh. India Acta Parasitol. 2021;66:236–52.
22. Bhat AH, Askary TH, Ahmad MJ, Suman, Aasha, Chaubey AK. Description of *Heterorhabditis bacteriophora* (Nematoda: Heterorhabditidae) isolated from hilly areas of Kashmir Valley. Egypt J Biol Pest Control. 2019;29:96.
23. Vanlalhlimpuia, Lalramliana, Lalramnghaki HC, Vanramliana. Morphological and molecular characterization of entomopathogenic nematode, *Heterorhabditis baujardi* (Rhabditida, Heterorhabditidae) from Mizoram, north eastern India. J Parasit Dis. 2018;42:341–9.
24. White GF. A method for obtaining infective nematode larvae from cultures. Science. 1927;66:302–3.
25. Leonar AL, Nimkingrat P, Aryal S, Martinez JG, Bhat AH, Sumaya NH. Natural association of the entomopathogenic nematode *Heterorhabditis indica* (Rhabditida: Heterorhabditidae) from the Philippines with the non-symbiotic bacterium *Ochrobactrum anthropi* (Proteobacteria: Brucellaceae). Egypt J Biol Pest Control. 2022;32:83.
26. Bhat AH, Istkhar, Chaubey AK, Půža V, San-Blas E. First report and comparative study of *Steinernema surkhetense* (Rhabditida: Steinernematidae) from subcontinental India. J Nematol. 2017;49:92–102.
27. Loulou A, Guerfali MM, Muller A, Bhat AH, Abolafia J, Machado RAR, et al. Potential of *Oscheius tipulae* nematodes as biological control agents against *Ceratitis capitate*. PLoS ONE. 2022;17:e0269106.
28. Bhat AH, Chaubey AK, Shokoohi E, Mashela PW. Study of *Steinernema hermaphroditum* (Nematoda, Rhabditida), from the West Uttar Pradesh. India Acta Parasitol. 2019;64:720–37.
29. Grisse AT. Rediscription ou modification de quelques techniques utilisees dans letude des nematodes phytoparasitaries. Meddelingen Rijksfaculteit landbouwweteschappen Bull. 1969;34:351–6.
30. Rana A, Bhat AH, Shokoohi E, Machado RAR. Morphological and molecular characterization *Heterorhabditis bacteriophora* nematodes isolated from Indian agricultural soils and their biocontrol potential. Zootaxa. 2020;4878:77–102.
31. Abolafia J. Extracción y procesado de nematodos de muestras de suelos de cuevas yotros hábitats. Monogr Biopg. 2022;16:6–17.
32. Siddiqi MR. Studies on *Discolaimus* spp. (Nematoda: Dorylaimidae) from India. J Zool Syst Evol Res. 1964;2:174–84.
33. Bharti L, Bhat AH, Chaubey AK, Abolafia J. Morphological and molecular characterisation of *Merlinius brevidens* (Allen, 1955) Siddiqi, 1970 (Nematoda: Rhabditida: Merlinidae) from India. J Nat Hist. 2020;54:1477–98.
34. Bhat AH, Chaubey AK, Hartmann J, Půža V. Notes on the morphology, bionomics, distribution and efficacy of *Steinernema siamkayai* (Rhabditida: Steinernematidae) from Western Uttar Pradesh. India Nematol. 2021;23:817–36.
35. Abolafia J. A low cost technique to manufacture a container to process meiofauna for scanning electron microscopy. Microsc Res Tech. 2015;78:771–6.
36. de Man JG. Die einheimischen, frei in der reinen Erde und im süssen Wasser lebende Nematoden. Tijdschrift Nederlandsche Dierkundige Vereeniging. 1880;5:1–104.
37. De Ley P, van de Velde MC, Mounport D, Baujard P, Coomans A. Ultrastructure of the stoma in Cephalobidae, Panagrolaimidae and Rhabditidae,

with a proposal for a revised stoma terminology in Rhabditida (Nematoda). Nematologica. 1995;41:153–82.

38. Abolafia J, Peña-Santiago R. On the identity of *Chiloplacus magnus* Rashid & Heyns, 1990 and *C. insularis* Orselli & Vinciguerra, 2002 (Rhabditida: Cephalobidae), two confusable species. Nematology. 2017;19:1017–34.

39. Bird AF, Bird J. The structure of nematodes, vol. 2. New York: Academic Press; 1991. p. 317.

40. Baldwin JG, Perry RN. Nematode morphology, sensory structure and function. In: Chen ZX, Dickson DW, Chen SY, editors. Nematology: advances and perspectives. Nematode morphology, physiology and ecology. Wallingford: CAB International; 2004. p. 197–201.

41. Dix I, Burnell AM, Griffin CT, Joyce SA, Nugent MJ, Downes MJ. The identification of biological species in the genus *Heterorhabditis* (Nematoda: Heterorhabditidae) by cross-breeding second-generation amphimictic adults. Parasitology 1992;104:509–18.

42. Suman B, Bhat AH, Aasha R, Chaubey AK, Abolafia J. Morphological and molecular characterization of *Distolabrellus veechi* (Rhabditida: Mesorhabditidae) from India. J Nematol. 2020;22:439–52.

43. Vrain TC, Wakarchuk DA, Lévesque AC, Hamilton RI. Intraspecific rDNA restriction fragment length polymorphism in the *Xiphinema americanum* group. Fund Appl Nematol. 1992;15:563–73.

44. Nadler SA, Bolotin E, Stock SP. Phylogenetic relationships of *Steinernema* Travassos, 1927 (Nematoda: Cephalobina: Steinernematidae) based on nuclear, mitochondrial and morphological data. Syst Parasitol. 2006;63:159–79.

45. Kuwata R, Yoshiga T, Yoshida M, Kondo E. Phylogenetic relationships of Japanese *Heterorhabditis* nematodes and their symbiotic *Photorhabdus* bacteria. Jpn J Nematol. 2007;37:39–50.

46. Bhat AH, Ameni L, Abolafia J, Machado RAR, Kallel S, Comparative morphological and molecular analyses of *Acrobeloides bodenheimeri* and *A. tricornis* Cobb. (Rhabditida, Cephalobidae) from Tunisia. Nematology. 1924;2023:207–26.

47. Dhakal M, Nguyen KB, Hunt DJ, Ehlers RU, Spiridonov SE, Subbotin SA. Molecular identification, phylogeny and phylogeography of the entomopathogenic nematodes of the genus *Heterorhabditis* Poinar, 1976: a multigene approach. Nematology. 2020;23:451–66.

48. Kimura MA. Simple method for estimating evolutionary rates of base substitutions through comparative studies of nucleotide sequences. J Mol Evol. 1980;16:111–20.

49. Hasegawa M, Kishino H, Yano T. Dating of the human-ape splitting by a molecular clock of mitochondrial DNA. J Mol Evol. 1985;22:160–74.

50. Nei M, Kumar S. Molecular evolution and phylogenetics. Oxford University Press; 2000. p. 352.

51. Tamura K, Stecher G, Kumar S. MEGA11: molecular evolutionary genetics analysis version 11. Mol Biol Evol. 2021;38:3022–7.

52. Edgar RC. MUSCLE: multiple sequence alignment with high accuracy and high throughput. Nucleic Acids Res. 2004;32:1792–7.

53. Chevenet F, Brun C, Bañuls AL, Jacq B, Christen R. TreeDyn: towards dynamic graphics and annotations for analyses of trees. BMC Bioinform. 2006;7:1–9.

54. Letunic I, Bork P. Interactive tree of life (iTOL) v3: An online tool for the display and annotation of phylogenetic and other trees. Nucleic Acids Res. 2016;44:W242–5.

55. Machado RAR, Ameni L, Bhat AH, Mastore M, Terrettaz C, Brivio MF, et al. *Acinetobacter nematophilus* sp. nov., *Alcaligenes nematophilus* sp. nov., *Enterobacter nematophilus* sp. nov., and *Kaistia nematophila* sp. nov., isolated from soil-borne nematodes and proposal for the elevation of *Alcaligenes faecalis* subsp. *faecalis*, *Alcaligenes faecalis* subsp. *parafaecalis*, and *Alcaligenes faecalis* subsp. *phenolicus* to the species level. Taxonomy. 2023;3:148–68.

56. Machado RAR, Bhat AH, Fallet P, Turlings TCJ, Kajuga J, Yan X, et al. *Xenorhabdus bovienii* subsp. *africana* subsp. nov., isolated from *Steinernema africanum* entomopathogenic nematodes. Int J Syst Evol Microbiol. 2023;73:1–9.

57. Bolger AM, Lohse M, Usadel B. Trimmomatic: a flexible trimmer for Illumina sequence data. Bioinform. 2014;30:2114–20.

58. Bankevich A, Nurk S, Antipov D, Gurevich AA, Dvorkin M, Kulikov AS, et al. SPAdes: a new genome assembly algorithm and its applications to single-cell sequencing. J Comput Biol. 2012;19:455–77.

59. Walker BJ, Abeel T, Shea T, Priest M, Abouelliel A, Sakthikumar S, et al. Pilon: an integrated tool for comprehensive microbial variant detection and genome assembly improvement. PLoS ONE. 2014;9:e112963.

60. Page AJ, Cummins CA, Hunt M, Wong VK, Reuter S, Holden MTG, et al. Roary: rapid large-scale prokaryote pan genome analysis. Bioinform. 2015;31:3691–3.

61. Price MN, Dehal PS, Arkin AP. FastTree: computing large minimum evolution trees with profiles instead of a distance matrix. Mol Biol Evol. 2009;26:1641–50.

62. Poinar GO Jr. Description and biology of a new insect parasitic rhabitoid, *Heterorhabditis bacteriophora* n. gen. n. sp. (Rhabditida; Heterorhabditidae n. family). Nematologica. 1976;21:463–70.

63. Li XY, Qi-Zhi L, Nermut J, Půža V, Mráček Z. *Heterorhabditis beicherriana* n. sp. (Nematoda: Heterorhabditidae), a new entomopathogenic nematode from the Shunyi district of Beijing, China. Zootaxa. 2012;3569:25–40.

64. Nguyen KB, Shapiro-Ilan DI, Mbata GN. *Heterorhabditis georgiana* n. sp. (Rhabditida: Heterorhabditidae) from Georgia, USA. Nematology. 2008;10:433–48.

65. Andaló V, Nguyen KB, Moino A. *Heterorhabditis amazonensis* n. sp. (Rhabditida: Heterorhabditidae) from Amazonas, Brazil. Nematology. 2006;8:853–67.

66. Edgington S, Buddie AG, Moore D, France A, Merino L, Hunt DJ. *Heterorhabditis atacamensis* n. sp. (Nematoda: Heterorhabditidae), a new entomopathogenic nematode from the Atacama Desert, Chile. J Helminthol. 2011;85:381–94.

67. Phan LK, Subbotin SA, Nguyen CN, Moens M. *Heterorhabditis baujardi* sp. n. (Rhabditida: Heterorhabditidae) from Vietnam with morphometric data for *H. indica* populations. Nematology. 2003;5:367–82.

68. Stock SP, Griffin CT, Burnell AM. Morphological characterisation of three isolates of *Heterorhabditis* Poinar, 1976 from the 'Irish group' (Nematoda: Rhabditida: Heterorhabditidae) and additional evidence supporting their recognition as a distinct species, *H. downesi* n. sp. Syst Parasitol. 2002;51:95–106.

69. Nguyen KB, Gozel U, Koppenhöfer HS, Adams BJ. *Heterorhabditis floridensis* n. sp. (Rhabditida: Heterorhabditidae) from Florida. Zootaxa. 2006;1177:1–19.

70. Liu J, Berry RE. *Heterorhabditis marelatus* n. sp. (Rhabditida: Heterorhabditidae) from Oregon. J Invertebr Pathol. 1996;67:48–54.

71. Poinar GO Jr, Jackson T, Klein M. *Heterorhabditis megidis* sp. n. (Heterorhabditidae: Rhabditidia), parasitic in Japanese beetle, *Popillia japonica* (Scarabidae: Coleoptera), in Ohio. Proc Helminthol Soc Wash. 1987;53:53–9.

72. Nguyen KB, Shapiro-Ilan DI, Stuart RJ, Mccoy CW, James RR, Adams BJ. *Heterorhabditis mexicana* n. sp. (Rhabditida: Heterorhabditidae) from Tamaulipas, Mexico, and morphological studies of the bursa of *Heterorhabditis* spp. Nematology. 2004;6:231–44.

73. Malan AP, Knoetze R, Tiedt L. *Heterorhabditis noenieputensis* n. sp. (Rhabditida: Heterorhabditidae), a new entomopathogenic nematode from South Africa. J Helminthol. 2014;88:139–51.

74. Malan AP, Nguyen KB, De Waal JY, Tiedt L. *Heterorhabditis safricana* n. sp. (Rhabditida: Heterorhabditidae), a new entomopathogenic nematode from South Africa. Nematology. 2008;10:381–96.

75. Shamseldean MM, Abou El-Sooud AB, Abd-Elgawad MMM, Saleh MM. Identification of a new *Heterorhabditis* species from Egypt, *Heterorhabditis taysearae* n. sp. (Rhabditida: Heterorhabditidae). Egyp J Biol Cont. 1996;6:129–38.

76. Poinar GO. Taxonomy and biology of Steinernematidae and Heterorhabditidae. In: Gaugler R, Kaya HK, editors. Entomopathogenic nematodes in biological control. Boca Raton: CRC Press; 1990. p. 23–61.

77. Bedding RA, Akhurst RJ. A simple technique for the detection of insect parasitic rhabditid nematodes in soil. Nematologica. 1975;21:109–10.

78. Askary TH, Bhat AH, Machado RAR, Ahmad MJ, Abd-Elgawad MMM, Khan AA, et al. Virulence and reproductive potential of Indian entomopathogenic nematodes against the larvae of the rice meal moth. Arch Phytopathol Plant Prot. 2023;55:2237–49.

79. Machado RAR, Bhat AH, Castaneda-Alvarez C, Askary TH, Půža V, Pagès S, et al. *Xenorhabdus aichiensis* sp. nov., *X. anantnagensis* sp. nov., and *X. yunnanensis* sp. nov., isolated from *Steinernema* entomopathogenic nematodes. Curr Microbiol. 2023;80:300.

Bhat *et al. Parasites & Vectors* (2023) 16:383

Page 28 of 28

80. Sudhaus W. Phylogenetic systematisation and catalogue of paraphyletic Rhabditidae (Secernentea, Nematoda). J Nematode Morphol Syst. 2011;14:113–78.

Publisher's Note

Springer Nature remains neutral with regard to jurisdictional claims in published maps and institutional affiliations.